Finite-temperature dynamical magnetic susceptibility of quasi-one-dimensional frustrated spin-$\frac{1}{2}$ Heisenberg antiferromagnets

Marc Bocquet,[1] Fabian H. L. Essler,[1] Alexei M. Tsvelik,[2] and Alexander O. Gogolin[3]
[1]*Department of Physics, Warwick University, Coventry CV4 7AL, United Kingdom*
[2]*Department of Physics, University of Oxford, 1 Keble Road, Oxford OX1 3NP, United Kingdom*
[3]*Department of Mathematics, Imperial College, 180 Queen's Gate, London SW7 2BZ, United Kingdom*
(Received 13 February 2001; revised manuscript received 14 May 2001; published 14 August 2001)

We study the dynamical response of frustrated, quasi-one-dimensional spin-$\frac{1}{2}$ Heisenberg antiferromagnets at finite temperatures. We allow for the presence of a Dzyaloshinskii-Moriya interaction. We concentrate on a model of weakly coupled planes of anisotropic triangular lattices. Combining exact results for the dynamical response of one-dimensional Heisenberg chains with a random-phase approximation in the frustrated interchain couplings, we calculate the dynamical susceptibility in the disordered phase. We investigate the instability of the disordered phase to the formation of collective modes. We find a very weak instability to the formation of incommensurate magnetic order and determine the ordering temperature and wave vector. We also determine the effects of uniform magnetic fields on the ordering transition.

DOI: 10.1103/PhysRevB.64.094425 PACS number(s): 75.10.−b, 75.25.+z, 75.40.−s

I. INTRODUCTION

A defining property of quasi-one-dimensional (1D) magnets is the weakness of the interchain coupling, whose presence nevertheless usually leads to three-dimensional ordering. It is natural to consider the ratio of the transition temperature T_c to the bandwidth of the excitation spectrum D as a quantitative measure of one dimensionality. In systems where $T_c/D \ll 1$ the ordering transition occurs in a state where spins on each chain are already highly ''collectivized.'' This means that a very significant proportion of the spectral weight is concentrated in a piece of the spin-spin correlation function, which is essentially one dimensional.[1–4] This suggests that the most natural approach to the problem of phase transitions in such systems is to treat them as instabilities,[5] driven by weak interchain interactions, of an ensemble of 1D chains. This approach utilizes the knowledge of the correlation functions of individual 1D chains, obtained by various nonperturbative methods. In this way one will automatically reproduce a distinct feature of quasi-1D magnets, namely the presence of a broad incoherent continuum in the dynamical structure factor. Hence this approach is quite different from the conventional spin-wave theory, which uses individual spins as elementary building blocks. Spin-wave theory is known to work well for the coherent (single-particle) parts of the spectra, but it is notoriously difficult to obtain the incoherent parts within this approach. Therefore it works poorly in one dimension, especially for spin-$\frac{1}{2}$ magnets, where the incoherence is very strong. The latter is due to the fact that excitations of a spin-$\frac{1}{2}$ Heisenberg chain carry quantum numbers different from those of spin waves.

Some of us have already applied the approach based on weakly coupled chains to describe the ordered phase of cubic lattice quasi-1D antiferromagnets[6] (see also Refs. 30 and 35). In the present work we apply an analogous method to the disordered phase and the ordering transition in quasi-1D, frustrated spin-$\frac{1}{2}$ antiferromagnets with Dzyaloshinskii-Moriya (DM) interaction. The effects of frustration on quantum magnets are very interesting and continue to attract much experimental[4,7–11] and theoretical[12–18] attention.

We focus on calculating the dynamical magnetic susceptibility $\chi(\omega,\vec{k})$, which is related to the dynamical structure factor $S(\omega,\vec{k})$ relevant for inelastic neutron-scattering experiments by

$$S^{\alpha\beta}(\omega,\vec{k}) = -\frac{1}{1-\exp(-\omega/T)}\ \mathrm{Im}\,\chi^{\alpha\beta}(\omega,\vec{k}). \qquad (1)$$

Note that throughout this paper we will mainly present plots of $-\mathrm{Im}\,\chi(\omega,\vec{k})$ rather than of the structure factor itself; the trivial prefactor in Eq. (1) can be easily restored if desired.

II. MODEL

Our work is inspired by the recent experiments on the frustrated spin-$\frac{1}{2}$ magnet Cs_2CuCl_4.[4,7–9] It was suggested in Refs. 4 and 9 that Cs_2CuCl_4 is described by a Heisenberg model on weakly coupled planes of anisotropic triangular lattices. Within the planes the exchange couplings are as indicated in Fig. 1.

Neighboring planes are coupled by a weak antiferromagnetic exchange J^z. In Cs_2CuCl_4 neighboring planes are

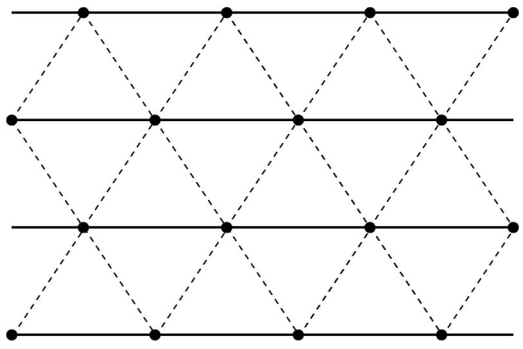

FIG. 1. Exchange paths within the planes: solid lines denote the strong exchange $J_\parallel$, dotted lines the weaker, frustrated exchange $J_\perp$.

slightly shifted with respect to one another, but in order to keep things simple we ignore this shift. The effective magnetic Hamitonian is thus given by

$$\mathcal{H}=\sum_k \mathcal{H}^{(k)}_{\rm plane}+\mathcal{H}^{(k,k+1)}_{\rm interplane},$$

$$\mathcal{H}^{(k)}_{\rm plane}=J_\parallel\sum_{i,j}\vec{S}_{i,j,k}\cdot\vec{S}_{i+1,j,k}+J_\perp\sum_{i,j}\vec{S}_{i,j,k}\cdot[\vec{S}_{i,j+1,k}+\vec{S}_{i-1,j+1,k}], \quad (2)$$

$$\mathcal{H}^{(k,k+1)}_{\rm interplane}=J_z\sum_{i,j}\vec{S}_{i,j,k}\cdot\vec{S}_{i,j,k+1}.$$

In the present work we analyze the model (2) in a quasi-1D framework. We choose to view the Hamiltonian (2) as spin-$\frac{1}{2}$ chains with exchange $J_\parallel$, coupled by a weaker, frustrating, nearest-neighbor exchange $J_\perp$ within a plane. Finally there is a very weak antiferromagnetic coupling J_z between neighboring planes.

Experimental estimates for the exchange couplings in Cs_2CuCl_4 are $J_\parallel=0.37$ meV, $J_\perp/J_\parallel\simeq 0.33(1)$, and $J_z/J_\parallel\approx 0.05$.[4,19] Although the interchain coupling $J_\perp/J_\parallel$ is considerable, the smallness of the ratio of transition temperature to bandwidth $T_c/\pi J_\parallel\approx 0.05$ indicates that the type of approach we are advocating might be applicable to Cs_2CuCl_4.

In addition to the exchange interactions present in Eq. (2) we allow for the presence of a DM interaction. Our motivation is once again the situation in Cs_2CuCl_4, where a DM interaction appears to be present[4,7–9,19] although it is not straightforward to estimate its magnitude. This is because the superexchange between two Cu spin-$\frac{1}{2}$ occurs through two Cl^- ligands and not a single one. One possible DM interaction that respects the crystal symmetry of Cs_2CuCl_4 is

$$\mathcal{I}_{\rm DM}=\sum_{i,j,k}\vec{D}\cdot[\vec{S}_{i,j,k}\times\vec{S}_{i+1,j,k}]. \quad (3)$$

Note that this form of the DM interaction only couples spins on the same chain. We mainly concentrate on a DM interaction of the type (3) but discuss how to treat more general forms in Sec. IX.

The outline of this paper is as follows. In Sec. III we review results for the dynamical susceptibility of a single spin-$\frac{1}{2}$ Heisenberg chain (with exchange anisotropy). In Sec. IV we study the effects of a frustrated interchain coupling between spin-$\frac{1}{2}$ chains. We determine the finite temperature dynamical structure factor by combining the results for single chains with a random-phase approximation in the interchain couplings. We show that an instability towards an incommensurate, ordered state develops at a critical temperature, which we determine as well. In Sec. V we study the effects of a uniform magnetic field. In Secs. VI, VII, and VIII we carry out the analogous program for spin-$\frac{1}{2}$ chains with DM interaction. In Sec. IX we show how to treat more general DM interactions within our calculational scheme. Section X contains a summary of our results and our conclusions.

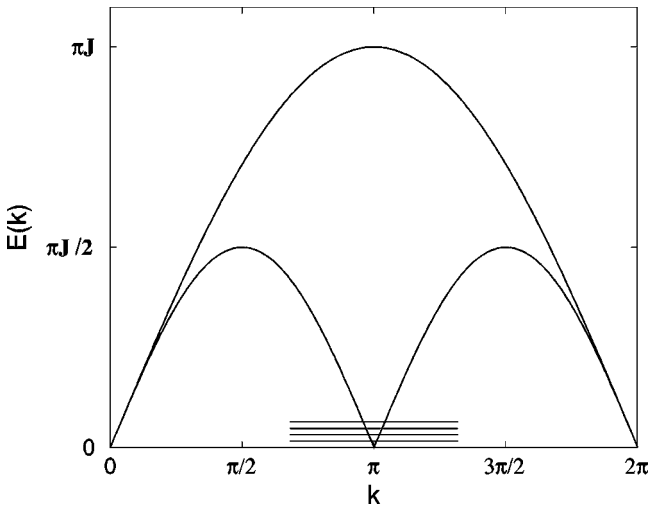

FIG. 2. Two-spinon dispersion for the isotropic Heisenberg chain. Also indicated are the sections for which we plot the dynamical susceptibility.

III. DYNAMICAL SUSCEPTIBILITY OF A SINGLE SPIN-$\frac{1}{2}$ *XXZ* CHAIN

Let us first consider a single Heisenberg chain with "*XY*-like" exchange anisotropy $0\leqslant\Delta\leqslant 1$,

$$\mathcal{H}_{XXZ}=J_\parallel\sum_j S^x_jS^x_{j+1}+S^y_jS^y_{j+1}+\Delta S^z_jS^z_{j+1}. \quad (4)$$

We will be particularly interested in the regime $\Delta\approx 1$. The spectrum of low-lying excitations consists of a two-spinon continuum[20] and is shown in Fig. 2 for the isotropic case $\Delta=1$. There are gapless modes at small momentum and at momentum π, where most of the spectral weight is concentrated. Spinons carry quantum number $S=\pm 1/2$ and no one-spinon excitations are present.

The large distance behavior of the finite temperature dynamical susceptibility can be determined by combining results obtained from the Bethe-Ansatz solution[21,22] of Eq. (4) with field theory techniques,[23–27]

$$\chi^{xx}(\tau,x)=(-1)^x A_x(\eta)\left[1-\left(\frac{\Lambda}{T}\right)^{4\eta-4}\right]^{1/2}\times\left[\frac{\left(\frac{\pi T}{u}\right)^2}{\sinh\left[\frac{\pi T}{u}(x-iu\tau)\right]\sinh\left[\frac{\pi T}{u}(x+iu\tau)\right]}\right]^{\eta/2}. \quad (5)$$

Here η is related to the exchange anisotropy Δ by

$$\eta=1-\arccos(\Delta)/\pi \quad (6)$$

and

$$u=J_\parallel a_0\sin(\pi\eta)/(2-2\eta) \quad (7)$$

is the spin velocity.

The nonuniversal amplitude $A_x(\eta)$ has been determined by Lukyanov and Zamolodchikov,[28]

$$A_x(\eta)=\frac{1}{8(1-\eta)^2}\left[\frac{\Gamma\left(\frac{\eta}{2(1-\eta)}\right)}{2\sqrt{\pi}\Gamma\left(\frac{1}{2(1-\eta)}\right)}\right]^{\eta} \times\exp\left[-\int_0^{\infty}\frac{dt}{t}\left(\frac{\sinh(\eta t)}{\sinh(t)\cosh[(1-\eta)t]}-\eta e^{-2t}\right)\right]. \tag{8}$$

Finally, Λ is a nonuniversal scale, which recently has been calculated in the isotropic case[29]

$$\Lambda/J_{\parallel}\approx 24.27. \tag{9}$$

The third factor on the right-hand side (RHS) of Eq. (5) stems from a renormalization-group (RG) improvement in the leading irrelevant perturbation to the conformally invariant scaling limit of Eq. (4).[26] There are further logarithmic corrections to Eq. (5), some of which have been calculated in the isotropic case[27] and lead to (small) corrections to some of the formulas we give below. We note that the RG improvement in Eq. (5) was done using the inverse temperature as the RG scale. It would be interesting to investigate the effects of working with two scales, i.e., the inverse temperature and the Euclidean distance. The RG improvements are important only in the vicinity of the isotropic point $\Delta=1$.

The frequency and momentum dependent dynamical susceptibility is obtained by Fourier transformation and analytic continuation of the time-ordered imaginary time correlation function (5) (see Refs. 24, 29, 31, and 32):

$$\chi^{xx}(\omega,\pi+k) =\Phi(T)\frac{\Gamma\left(\frac{\eta}{4}-i\frac{\omega-uk}{4\pi T}\right)}{\Gamma\left(1-\frac{\eta}{4}-i\frac{\omega-uk}{4\pi T}\right)}\frac{\Gamma\left(\frac{\eta}{4}-i\frac{\omega+uk}{4\pi T}\right)}{\Gamma\left(1-\frac{\eta}{4}-i\frac{\omega+uk}{4\pi T}\right)}. \tag{10}$$

Here $\Phi(T)$ is given by

$$-A_x(\eta)\frac{\sin\left(\pi\frac{\eta}{2}\right)\Gamma^2\left(1-\frac{\eta}{2}\right)}{u}\left[1-\left(\frac{\Lambda}{T}\right)^{4\eta-4}\right]^{1/2}\left[\frac{u}{2\pi T}\right]^{2-\eta}. \tag{11}$$

The result (10) is valid for momentum transfers close to the antiferromagnetic wave number $q\approx\pi$, low energies $\omega/J_{\parallel}\ll 1$, and low temperatures $T/J_{\parallel}\ll 1$.

The result for the isotropic point $\Delta=1$ is obtained by taking the limit $\eta\to 1$. In this limit A_x diverges and $\sqrt{1-(\Lambda/T)^{4\eta-4}}$ goes to zero according to

$$A_x(\eta)\to\frac{1}{2(2\pi)^{3/2}\sqrt{1-\eta}}, \tag{12}$$

$$\sqrt{1-(\Lambda/T)^{4\eta-4}}\to 2\sqrt{1-\eta}\sqrt{\ln(\Lambda/T)}, \tag{13}$$

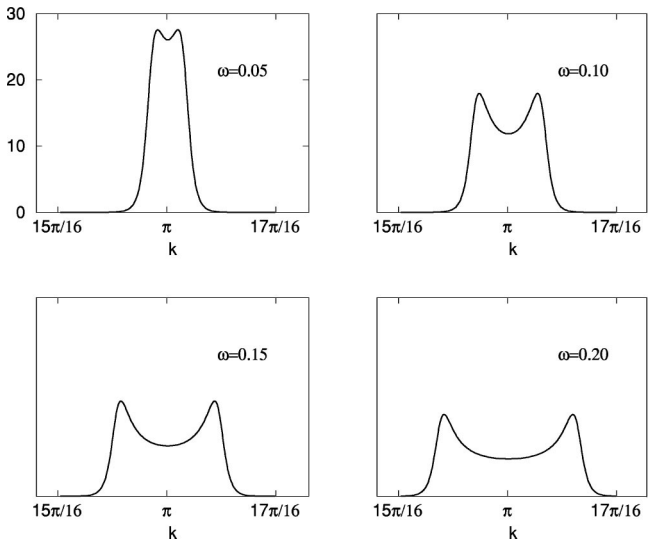

FIG. 3. Imaginary part of the dynamical susceptibility $-\mathrm{Im}\,\chi^{xx}(\omega,k)$ in units of $1/J_{\parallel}$ for the isotropic Heisenberg chain as a function of q for four different values of $\omega/J_{\parallel}$ at a temperature of $k_BT/J_{\parallel}=0.01$.

so that their product tends to $\sqrt{\ln(\Lambda/T)}/(2\pi)^{3/2}$.

In Fig. 3 we show the imaginary part of the transverse susceptibility in the isotropic case for the ''constant-energy scans'' indicated in Fig. 2. The two-spinon continuum is clearly visible. The maxima at fixed frequency occur close to the boundaries of the two-spinon continuum.

The longitudinal dynamical susceptibility is given by

$$\chi^{zz}(\omega,\pi+k) =\Phi'(T)\frac{\Gamma\left(\frac{1}{4\eta}-i\frac{\omega-uk}{4\pi T}\right)}{\Gamma\left(1-\frac{1}{4\eta}-i\frac{\omega-uk}{4\pi T}\right)}\frac{\Gamma\left(\frac{1}{4\eta}-i\frac{\omega+uk}{4\pi T}\right)}{\Gamma\left(1-\frac{1}{4\eta}-i\frac{\omega+uk}{4\pi T}\right)}, \tag{14}$$

where $\Phi'(T)$ is given by[33]

$$\Phi'(T)=-A_z(\eta)\frac{\sin(\pi/2\eta)\Gamma^2(1-1/2\eta)}{u}\left[\frac{u}{2\pi T}\right]^{2-1/\eta} \times\left[1-\left(\frac{\Lambda}{T}\right)^{2\eta-2}\right]^{1/2}\left[1+\left(\frac{\Lambda}{T}\right)^{2\eta-2}\right]^{-3/2},$$

$$A_z(\eta)=\frac{2}{\pi^2}\left[\frac{\Gamma\left(\frac{\eta}{2(1-\eta)}\right)}{2\sqrt{\pi}\Gamma\left(\frac{1}{2(1-\eta)}\right)}\right]^{1/\eta} \times\exp\left[\int_0^{\infty}\frac{dt}{t}\left(\frac{\sinh[(2\eta-1)t]}{\sinh(\eta t)\cosh[(1-\eta)t]} -\frac{2\eta-1}{\eta}e^{-2t}\right)\right]. \tag{15}$$

For $\Delta<1$ the longitudinal structure factor at low energies is weaker than the transverse one. In Fig. 4 we compare the transverse and longitudinal susceptibilities for an XXZ chain with $\Delta=0.9$.

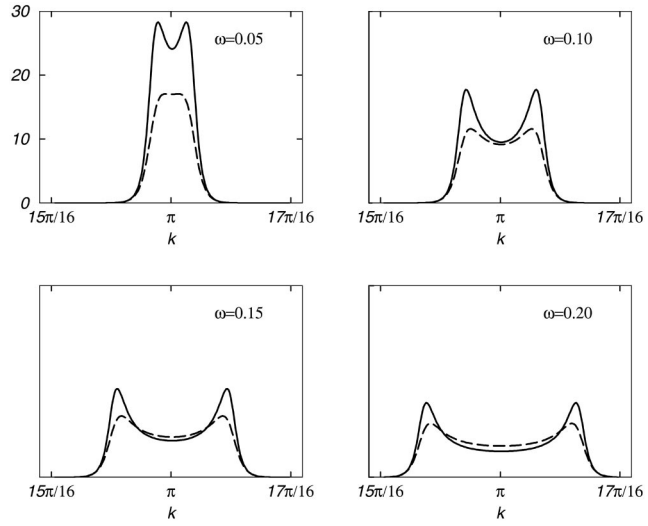

FIG. 4. Minus the imaginary part of the transverse (full line) versus longitudinal dynamical susceptibility (dashed line) in the anisotropic Heisenberg XXZ chain with $\Delta=0.9$.

IV. DYNAMICAL SUSCEPTIBILITY FOR COUPLED HEISENBERG CHAINS

Let us now take into account the interchain couplings $J_\perp$ and J_z. We do this by a random-phase approximation (RPA),[34,35] which in the present context can be understood as the leading term of an expansion in the inverse coordination number of the lattice. The dynamical susceptibility of (three-dimensionally) coupled chains are of the form

$$\chi^{\alpha\alpha}_{3d}(\omega,\vec{k})=\frac{\chi^{\alpha\alpha}(\omega,k)}{1-2J(k,k_y,k_z)\chi^{\alpha\alpha}(\omega,k)}, \tag{16}$$

where $\alpha=x,y,z$ and $\chi^{\alpha\alpha}(\omega,k)$ is the dynamical susceptibility of a single chain. The Fourier transform of the interchain spin-spin couplings $J(k,k_y,k_z)$ is given by

$$J(k_x,k_y,k_z)=J_z\cos(k_z)+J_\perp[\cos(k_y)+\cos(k_x-k_y)]. \tag{17}$$

We recall that we have assumed the coupling along the z direction (between planes) to be antiferromagnetic, i.e. unfrustrated. We can recover the results for a weak, frustrated coupling between planes with $J_z \ll J_\perp$ by simply setting $J_z=0$ in our formulas. Whenever we thus refer to $J_z=0$ in the following, this should be understood as corresponding to a weak, frustrated coupling along the z direction.

In the experiments on Cs_2CuCl_4 the dynamical structure factor was measured for momentum transfers along the chain direction. We therefore concentrate on such momentum transfers in the framework of our approach.

The elementary cell and the first Brillouin zone of the planar triangular lattice are shown in Fig. 5. If one probes the magnetic properties of the crystal along the direction of the spin chains, the wave-vector transfer follows the trajectory $k_y=k_x/2 \mod (2\pi)$ in the first Brillouin zone and has been represented by three arrows in Fig. 5. We see that the wave-number transfer along the chain direction varies in the interval $[0,4\pi]$.

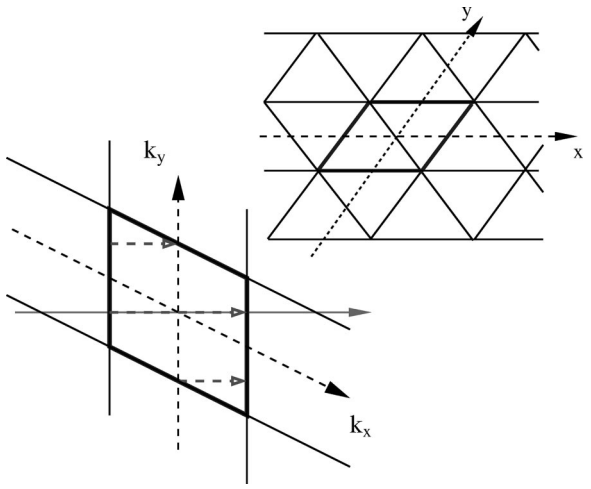

FIG. 5. Primitive cell of the triangular lattice and corresponding first Brillouin zone. Wave numbers corresponding to momentum transfer along the chain direction are indicated by arrows.

In Figs. 6 and 7 we plot (minus) the imaginary part of $\chi^{xx}_{3d}(\omega,\vec{k})$ for momentum transfers along the chain direction for four different values of $\omega/J_\parallel$. We have chosen parameters such that $J_\perp/J_\parallel=0.1$, $T/J_\parallel=0.01$, $J^z=0$ and $J_\perp/J_\parallel=0.1$, $T/J_\parallel=0.02$, $J^z=0.01$, respectively. In both cases the temperature is chosen to be above the transition to an ordered state (see below) as it must for our approach to apply.

Figures 6 and 7 show very clearly that the main effect of the frustrated interchain coupling is to make the line shape *asymmetric*. The susceptibility of uncoupled chains for momentum transfer along the chain direction is symmetric

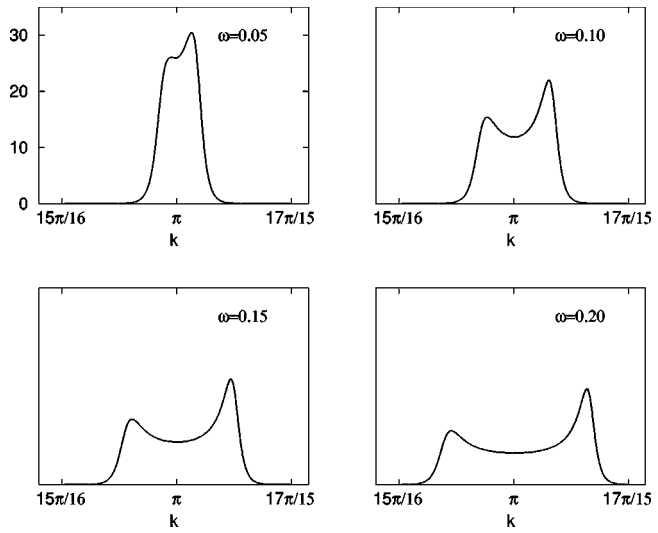

FIG. 6. Imaginary part of the dynamical susceptibility $-\mathrm{Im}\,\chi^{xx}_{3d}(\omega,\vec{k})$ for momentum transfers along the chain direction. The parameters are $J_\perp/J_\parallel=0.1$, $T/J_\parallel=0.01$, and $J^z=0$. We see that the frustrated interchain coupling leads to an asymmetric line shape.

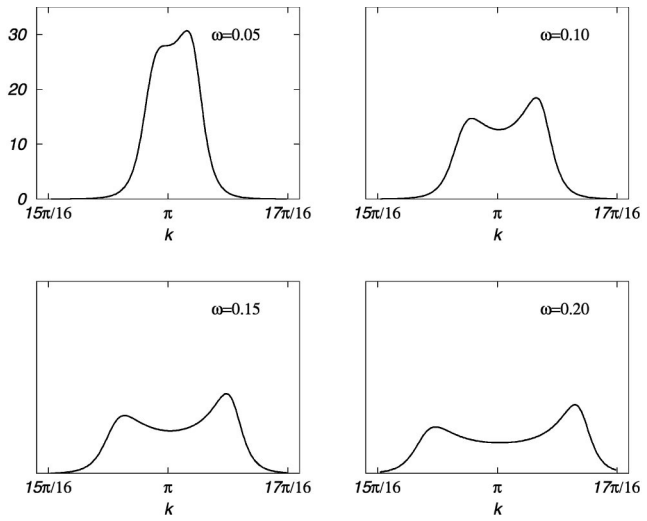

FIG. 7. $-\mathrm{Im}\,\chi^{xx}_{3d}(\omega,\vec{k})$ for momentum transfers along the chain direction. The parameters are $J_\perp/J_\parallel=0.1$, $T/J_\parallel=0.02$, and $J^z/J_\parallel=0.01$.

around the antiferromagnetic wave number $k=\pi$ as can be seen, for example, in Fig. 3. This symmetry is lost when the interchain coupling is taken into account. The asymmetry increases with increasing $J_\perp$. The curves for $J_z=0$ and $J_z=0.01$ are qualitatively similar. Another important feature of the imaginary part of the dynamical susceptibility is that it looks *incommensurate*—the maximum occurs at an incommensurate value of the momentum transfer along the chain direction. This is most easily seen in a contour plot such as Fig. 8, where the dynamical structure factor $S^{xx}(\omega,\vec{k})$ is shown as a function of energy and momentum transfer along the chain direction. The dynamical structure factor in the disordered phase of Cs_2CuCl_4 displays both incommensurabilities and an asymmetric structure.[4]

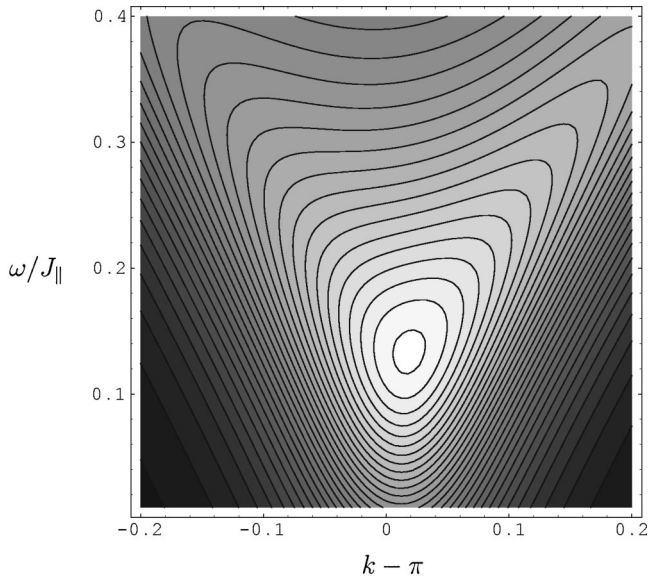

FIG. 8. Dynamical structure factor $S^{xx}(\omega,\vec{k})$ for momentum transfers along the chain direction. The parameters are $J_\perp/J_\parallel=0.2$, $T/J_\parallel=0.05$, and $J^z/J_\parallel=0.02$.

A. Instability condition and critical temperature

The RPA expression for the dynamical susceptibility is valid in the disordered phase, i.e., at temperatures above the transition to an ordered state. One can obtain an estimate for the ordering temperature T_c by considering the condition for an instability to develop in form of a zero-frequency pole in $\chi_{3d}(\omega,\vec{k})$.[34,35] This pole indicates that the system is unstable with respect to developing collective modes. In the case of an antiferromagnet on a cubic lattice the instability signals the spontaneous breakdown of spin rotational symmetry via the emergence of Néel order and the collective modes are the corresponding Goldstone modes (spin waves). For the case of a quasi-1D antiferromagnet on a cubic lattice, the critical temperature obtained in this way is comparable to the experimentally measured Néel temperature for $KCuF_3$.[35,2] The leading corrections in the inverse coordination number of the lattice can be calculated as well.[36] In our case the instability condition reads

$$2J(k,k_y,k_z)\chi^{\alpha\alpha}(0,k)\big|_{T=T_c}=1, \tag{18}$$

where $\alpha=x,z$. We find that for $\alpha=z$ the condition (18) leads to a weaker instability, i.e., occurring at a lower temperature, except in the case of zero exchange anisotropy. We therefore concentrate on $\alpha=x$ from now on. The instability will develop at the maximum of $J(k,k_y,k_z)\,\chi^{xx}(0,k)$. The maximum of the susceptibility of a single chain $\chi^{xx}(0,k)$ occurs at $k=\pi$, but because $J(k,k/2,0)=0$ vanishes at this point the maximum of $J\chi^{xx}$ will be shifted away from the antiferromagnetic wave number.

Extremizing $J(k,k_y,k_z)\chi^{xx}(0,k)$ with respect to k_y and k_z yields $k_y=k/2 \mod(2\pi)$ and $k^z=\pi$. Setting $k_y=k/2$, $k_z=\pi$ we find that the maximum of the resulting expression occurs at a value $k=\pi+k_0$ such that

$$\frac{\pi\sinh(uk_0/2T_c)}{\cosh(uk_0/2T_c)-\cos\left(\frac{\pi\eta}{2}\right)}+\frac{2\pi T_c}{u}\frac{\cos(k_0/2)}{J_z/J_\perp+2\sin(k_0/2)}$$
$$-2\,\mathrm{Im}\,\Psi\left(\frac{\eta}{4}+i\frac{uk_0}{4\pi T_c}\right)=0, \tag{19}$$

where $\Psi(x)$ is the digamma function. Equations (19) and (18) with $k=\pi+k_0$, $k_y=(\pi+k_0)/2$, $k_z=\pi$ constitute two equations for the two unknowns k_0 and T_c. Let us emphasize that a solution with $k_0\neq 0$ corresponds to an instability at an incommensurate wave number $\pi+k_0$. This suggests that the resulting order occurs along the chain direction with characteristic wave number $\pi+k_0$.

In general, Eqs. (18) and (19) can only be solved numerically, which is easily done. An exception is the special case $J_z=0$ and $\Delta=1$ (isotropic point), for which we can derive analytic expressions.

1. Isotropic point ($\eta=1$)

In the absence of an exchange anisotropy Eq. (19) simplifies further,

$$\frac{2\pi T_c}{uk_0}+\pi\tanh(uk_0/2T_c)-2\,\mathrm{Im}\,\Psi\left(\frac{1}{4}+i\frac{uk_0}{4\pi T_c}\right)=0. \tag{20}$$

Solving for $x_0=k_0/(4\pi T_c)$, we find

$$x_0=\frac{\hbar u}{a_0}\frac{k_0}{4\pi T_c}\approx\pm 0.31, \tag{21}$$

where we have restored units (k_0 is measured in units of the lattice spacing a_0 and T in units of k_B). We note that $k_0\neq 0$, which means that the instability develops at an *incommensurate* wave number close to π.

The remaining Eq. (18) then becomes

$$\begin{aligned}2J(k_0,0,0)\chi(0,k_0)&=-2[J_z+2J_\perp\sin(k_0/2)]\chi(0,k_0)\\&=\frac{1}{(2\pi)^{3/2}}\left|\frac{\Gamma\left(\frac{1}{4}+ix_0\right)}{\Gamma\left(\frac{3}{4}+ix_0\right)}\right|^2\\&\quad\times\left(\frac{J_z}{T_c}+\frac{4\pi x_0 J_\perp a_0}{\hbar u}\right)\sqrt{\ln(\Lambda/T_c)}\\&\approx 0.25\left(\frac{J_z}{T_c}+8x_0\frac{J_\perp}{J_\parallel}\right)\sqrt{\ln(\Lambda/T_c)}=1.\end{aligned} \tag{22}$$

Here we have used the result for the spin velocity of the isotropic Heisenberg spin-$\frac{1}{2}$ chain $u=\pi J_\parallel a_0/2$.

Let us first ignore the effects of the coupling J_z between planes. This case would correspond to a situation where the coupling in z direction is also frustrated, but much smaller than $J_\perp$. The critical temperature and ordering wave number are then given by

$$T_c\approx\Lambda\exp[-2.60(J_\parallel/J_\perp)^2], \tag{23}$$

$$|k_0|\approx 2.48\frac{\Lambda}{J_\parallel}\exp[-2.60(J_\parallel/J_\perp)^2]. \tag{24}$$

These clearly show that the instability due to the frustrated interchain coupling is *extremely weak*. First, the critical temperature is orders of magnitude lower than its counterpart for the square lattice. This is an indication how weak the tendency to order is on a frustrated lattice. Even for a large interchain coupling $J_\parallel/J_\perp=0.4$, the critical temperature is only $T_c\approx 9.10^{-6}$ K. The ordering wave number is similarly small. Our results should be compared to the zero-temperature results for the ordering wave number of Refs. 14 and 15. The authors of Ref. 14 used linked-cluster expansion methods to study ground-state properties and excited states at zero temperature of a rather general frustrated model, which contains the anisotropic triangular lattice as a special case. They obtain numerically (in their notations our antiferromagnetic wave number corresponds to $\pi/2$)

$$q\simeq\arccos\left(\frac{1}{4-6J_\parallel/J_\perp}\right), \tag{25}$$

which yields a much larger incommensuration than our result. In Ref. 15 a Heisenberg model on an anisotropic triangular lattice was studied by enlarging the spin-rotational symmetry group from SU(2) to Sp(N) and then carrying out a large-N expansion. It was concluded that for weak $J_\perp<0.125J_\parallel$ there is no incommensuration at all. Given the approximate nature of our results, they are certainly compatible with such a scenario.

In our approach the instability in the SU(2) invariant case is actually caused by the marginally irrelevant current-current interaction that gives rise to logarithmic corrections. The weakness of the instability is due to the fact that it is caused by precisely these logarithmic corrections.

TABLE I. Transition temperatures $t_c=T_c/J_\parallel$ and ordering wave numbers k_0 for isotropic exchange interaction and various values of the frustrated ($J_\perp$) and antiferromagnetic (J^z) interchain couplings.

$J_z/J_\parallel$	$J_\perp/J_\parallel=0.1$	$J_\perp/J_\parallel=0.2$	$J_\perp/J_\parallel=0.3$
0	$t_c=2.910^{-112}$	$t_c=1.410^{-27}$	$t_c=6.910^{-11}$
	$k_0=7.310^{-112}$	$k_0=3.610^{-27}$	$k_0=1.710^{-10}$
0.01	$t_c=0.015$	$t_c=0.017$	$t_c=0.019$
	$k_0=0.005$	$k_0=0.011$	$k_0=0.019$
0.02	$t_c=0.029$	$t_c=0.032$	$t_c=0.036$
	$k_0=0.009$	$k_0=0.020$	$k_0=0.034$
0.04	$t_c=0.056$	$t_c=0.060$	$t_c=0.066$
	$k_0=0.017$	$k_0=0.036$	$k_0=0.060$
0.1	$t_c=0.13$	$t_c=0.14$	$t_c=0.15$
	$k_0=0.036$	$k_0=0.076$	$k_0=0.13$

2. General case

In the general case $J_z\neq 0$ it is not possible to obtain simple analytic expressions like Eqs. (23) and (24) for T_c and k_0, respectively, and we have to resort to a numerical solution of (18) and (19). We present the results for various values of J_z and $J_\perp$ in Table I.

We see that increasing J_z leads to a significant increase of the transition temperature *and* the ordering wave number, whereas increasing the frustrated coupling $J_\perp$ mainly increases the value of k_0. The interesting observation is that a purely antiferromagnetic coupling between the chains leads not only to a higher transition temperature (as expected), but also to a significantly larger value of the ordering wave number. If we take values similar to those for Cs_2CuCl_4 ($J_\perp/J\approx 0.33$, $J_z/J_\parallel\approx 0.05$) we obtain a transition temperature of $t_c=0.084$ and an incommensurability of $k_0=0.083$. If we take subleading corrections in the RG improvement into account[27] these values increase to $t_c=0.108$ and $k_0=0.104$, respectively.

These values (which should be taken with a degree of caution as $J_\perp$ is not small) are roughly comparable to what is observed for Cs_2CuCl_4,[4] where $t_c\approx 0.145$ and $k_0\approx 0.186$. As is shown in Sec. VII, the presence of a DM interaction can further increase t_c and k_0.

We may also study the effects of an exchange anisotropy $\Delta<1$ along the z direction is spin space [the chain Hamiltonian then is given by Eq. (4)]. The analysis is completely

analogous the isotropic case. We find that the anisotropy enhances both the transition temperature and the ordering wave number. For example, for $\Delta=0.8$, $J_z=0.01J_\parallel$, and $J_\perp=0.1J_\parallel$ we obtain $k_0=0.007$, $t_c=0.023$. For $\Delta=0.5$, $J_z=0.01J_\parallel$, and $J_\perp=0.1J_\parallel$ we have $k_0=0.013$, $t_c=0.033$.

V. THE EFFECT OF A UNIFORM MAGNETIC FIELD

As we have mentioned in the introduction, the inspiration for the present work are the observed properties of Cs_2CuCl_4. The effects of an applied magnetic field[7,4] are particularly intriguing. Let us therefore turn to the study of the effects of a uniform field on the dynamical susceptibility, ordering temperature, and ordering wave number. To this end, we must modify the dynamical susceptibility of a single chain by taking into account the effect of the field. This can be done by utilizing exact results obtained by the Bethe Ansatz[22] (see the Appendix of Ref. 37 for a brief summary). For simplicity we consider the case of a single, isotropic Heisenberg XXX chain ($\Delta=1$). In zero field we have full spin rotational symmetry and transverse and longitudinal susceptibilites coincide. There are gapless, transverse, and longitudinal excitations at $k=\pi$ and the spectral weight of the dynamical structure factor is concentrated in the region around $k=\pi$. Application of a magnetic field breaks the symmetry between transverse and longitudinal susceptibilities.

The transverse susceptibility at low energies is dominated by the contribution from the gapless states at $k=\pi$ in Fig. 9(a), whereas the most important contributions to the longitudinal susceptibility at low energies comes from the gapless states at the incommensurate wave numbers $\pi\pm\delta(H)$ in Fig. 9(b).

At $T=0$ the large-distance asymptotics of the transverse spin-spin correlation functions in real space is

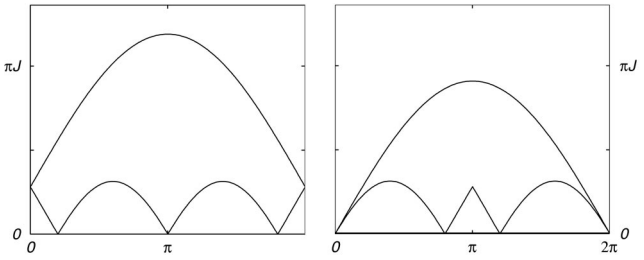

FIG. 9. Two-spinon continuum for the isotropic Heisenberg chain in a magnetic field. (a) States with $\Delta S^z=1$; (b) states with $\Delta S^z=0$.

$$\langle S^x(\tau,y)S^x(0,0)\rangle \simeq A_x(H)\frac{(-1)^{y/a_0}}{|y+iu(H)\tau|^{\eta(H)}}. \qquad (26)$$

The magnetic-field-dependent spin velocity $u(H)$ and exponent $\eta(H)$ can be calculated to high precision from the Bethe Ansatz by solving certain linear integral equations.[22] The amplitude $A_x(H)$ is not known analytically but has very recently been calculated numerically for several values of H using a density-matrix renormalization-group algorithm.[38]

The asymptotic behavior (26) holds for distances $|\tau+iy/u(H)|$ large compared to $1/H$. The asymptotic behavior of the spin-spin correlator at very large distances is changed by the application of a magnetic field, but at ''intermediate'' distances the field does not play the same role. In order to utilize Eq. (26) we therefore need sufficiently large magnetic fields. This is the case we are interested in. For small fields Eq. (26) holds only at extremely large distances and it is better to take the field into account in RG improved perturbation theory.

The dynamical susceptibility can now be determined by Fourier transforming Eq. (26) and then analytically continuing the result to real frequencies. The calculation is analogous to the one in zero field[35] and one obtains the following result for the low-energy transverse susceptibility of a single, isotropic Heisenberg XXX chain ($\Delta=1$) in a magnetic field

$$\chi^{xx}(\omega,\pi-k,H)=\Phi(T,H)\frac{\Gamma\left(\frac{\eta(H)}{4}-i\frac{\omega-u(H)k}{4\pi T}\right)}{\Gamma\left(1-\frac{\eta(H)}{4}-i\frac{\omega-u(H)k}{4\pi T}\right)}\frac{\Gamma\left(\frac{\eta(H)}{4}-i\frac{\omega+u(H)k}{4\pi T}\right)}{\Gamma\left(1-\frac{\eta(H)}{4}-i\frac{\omega+u(H)k}{4\pi T}\right)}, \qquad (27)$$

where $|k|\ll 1$ and $\Phi(T,H)$ is given by

$$\Phi(T,H)=-A_x(H)\frac{\sin[\pi\eta(H)/2]\Gamma^2[1-\eta(H)/2]}{u(H)}\left[\frac{u(H)}{2\pi T}\right]^{2-\eta(H)}. \qquad (28)$$

The presently available results for the unknowns in Eqs. (26) and (27) are summarized in Table II.

As noted above, the result (27) is least reliable at low fields as it is obtained by Fourier transforming the large-distance asymptotics of the real-space correlation function.

Using the results summarized in Table II in Eq. (27) we obtain the transverse susceptibility for a single chain. This result can now again be combined with an RPA treatment of the interchain couplings to obtain an expression for the susceptibility of the quasi-1D. Following the same steps as in the absence of a field we can determine a critical temperature and ordering wave number.

TABLE II. Magnetization $M(H)$, spin velocity $u(H)$, exponent $\eta(H)$, and amplitude $A_x(H)$ for different values of the uniform magnetic field H.

M(H)	$H/J_\parallel$	$A_x(H)$	$\eta(H)$	$u(H)/J_\parallel a_0$
0.05	0.422	0.121	0.837	1.501
0.10	0.792	0.120	0.782	1.398
0.15	1.109	0.118	0.735	1.259
0.20	1.373	0.117	0.692	1.093
0.25	1.585	0.112	0.653	0.911
0.30	1.748	0.106	0.617	0.721
0.35	1.866	0.095	0.584	0.529
0.40	1.944	0.081	0.554	0.342
0.45	1.987	0.061	0.526	0.165

In Fig. 10 we plot the ordering temperature and wave number as a function of the applied field. We see that at first both increase with the field, but $T_c(H)$ eventually goes through a maximum and then decreases. This is in qualitative agreement with what has been observed for Cs_2CuCl_4. If we switch on an exchange anisotropy along the z direction in spin space the qualitative behavior of the T_c and k_0 as functions of H remain the same.

So far we have only considered the transverse susceptibility. In the presence of a field we still have to check for possible instabilities in the longitudinal susceptibility as the maxima of $\chi^{xx}(0,k,H)$ and $\chi^{zz}(0,k,H)$ occur for different values of k. It is important to note that the physical nature of a longitudinal instability is very different from that of a transverse one. The latter is associated with the spontaneous breakdown of the spin rotational symmetry around the direction of the magnetic field, whereas a longitudinal instability does not break any continuous symmetries, but rather corresponds to the formation of a spin-density wave in the ground state.

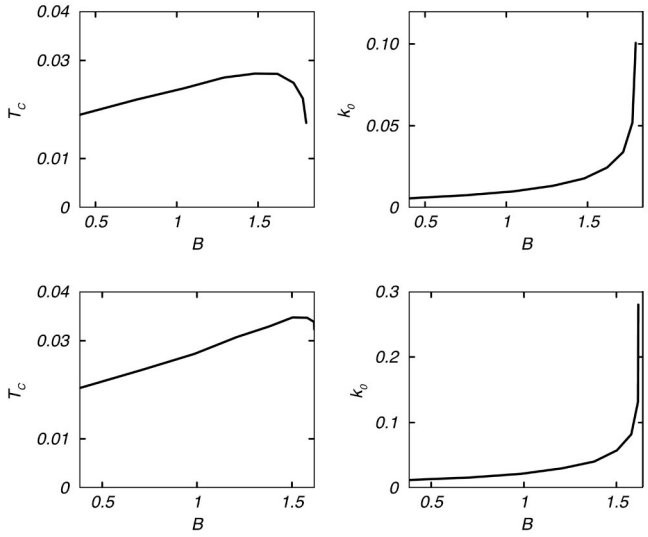

FIG. 10. Upper two graphs: critical temperature T_c and ordering wave number k_0 extracted from the transverse susceptibility as functions of the applied field $B=H/J_\parallel$ for isotropic Heisenberg chains coupled by a frustrated in-plane coupling $J_\perp=0.1J_\parallel$ and antiferromagnetic inter-plane coupling $J_z=0.01J_\parallel$. Lower two graphs: the same for $J_\perp=0.2J_\parallel$.

The longitudinal susceptibility in a field can be calculated along the same lines as outlined above for the transverse ones. However, the longitudinal real-space correlation function decays *faster* with distance as the field is increased. Therefore it is likely that Fourier transforming the large-distance asymptotics leads to a less reliable result than for the transverse susceptibilities. It would be very interesting to investigate this issue by numerical methods. Fourier transformation of the large-distance asymptotics and analytical continuation yields

$$\chi^{zz}(\omega,\pi\pm\delta-k,H)=\Phi'(T,H)\,\frac{\Gamma\left(\frac{1}{4\eta(H)}-i\frac{\omega-u(H)k}{4\pi T}\right)}{\Gamma\left(1-\frac{1}{4\eta(H)}-i\frac{\omega-u(H)k}{4\pi T}\right)}\,\frac{\Gamma\left(\frac{1}{4\eta(H)}-i\frac{\omega+u(H)k}{4\pi T}\right)}{\Gamma\left(1-\frac{1}{4\eta(H)}-i\frac{\omega+u(H)k}{4\pi T}\right)}, \tag{29}$$

where $\delta=2\pi M(H)$ and $\Phi'(T,H)$ is given by

$$\Phi'(T,H)=-A_z(H)\,\frac{\sin[\pi/2\eta(H)]\Gamma^2[1-1/2\eta(H)]}{u(H)}\left[\frac{u(H)}{2\pi T}\right]^{2-1/\eta(H)}. \tag{30}$$

The amplitude $A_z(H)$ is again known numerically,[38] so that we can repeat the analysis carried out above for the transverse susceptibility. We find that in general an instability in the longitudinal susceptibility exists at a critical temperature comparable to the one for the transverse instability. The corresponding characteristic wave number k_0 is located in the vicinity of $\pi\pm\delta=\pi\pm2\pi M(H)$, where $M(H)$ is the magnetization of uncoupled chains. Note that $\pi\pm\delta$ are the points where incommensurable soft modes exist in the $\Delta S^z=0$ sector of the excitation spectrum of individual chains [see Fig. 9(b)]. For large values of the applied field H, $\pi\pm\delta$ approach 0 and 2π, respectively. We note that in this regime the further complication arises that it is no longer appropriate to neglect the contributions [as has been done in Eq. (29)] of the smooth, nonoscillating terms in the spin-spin correlation functions.

As a function of the applied field H, the transition temperature of the longitudinal instability $t_c^{\rm long}(H)$ first increases, goes through a maximum and then decreases again. This is similar to what we obtained for the transverse instability. However, in contrast to the transverse instability the maximum of $t_c^{\rm long}(H)$ occurs at small magnetization.

Which instability is dominant is rather sensitive to the values of $J_\perp$, J_z and the applied field H. For $J_\perp = 0.1J_\parallel$, $J_z = 0.01J_\parallel$ we find that the transverse instability occurs at a higher temperature except for small fields, where the longitudinal susceptibility appears to dominate. On the other hand, as we have pointed out above, for small fields our results for the Fourier transforms are least reliable.

So far we have worked with a spin rotationally symmetric Hamiltonian. Let us now consider the effects of an exchange anisotropy. We have to distinguish two cases, depending whether or not the applied field is along the direction of the exchange anisotropy. In the former case the analysis is completely analogous to the spin rotationally symmetric case and we find a behavior $T_c(H)$ and $k_0(H)$ very similar to Fig. 10. The transition temperature increases with increasing field, goes through a maximum, and eventually decreases again.

Let us now turn to the case where we have an exchange anisotropy in the z direction and apply the field along the x direction. The effect of the magnetic field is now to generate an excitation gap. This can be seen as follows. The chain Hamiltonian is

$$\mathcal{H}_{XXZ,H} = J_\parallel \sum_j S_j^x S_{j+1}^x + S_j^y S_{j+1}^y + \Delta S_j^z S_{j+1}^z + H \sum_j S_j^x = \mathcal{H}_0 + \mathcal{H}_1, \tag{31}$$

where $\mathcal{H}_0$ is the Hamiltonian of the anisotropic spin-$\frac{1}{2}$ chain and

$$\mathcal{H}_1 = H \sum_j S_j^x. \tag{32}$$

Let us study the effect of the perturbing operator by bosonizing at the critical point defined by $\mathcal{H}_0$ and then perturbing this fixed point theory by Eq. (32). The bosonized form of $\mathcal{H}_0$ is

$$\mathcal{H}_0 = \frac{1}{2} \int dx [(\partial_x \Theta)^2 + (\partial_x \Phi)^2], \tag{33}$$

where Φ is a canonical bosonic field and Θ is the dual field. The uniform part of the x component of the magnetization is given by the product of two operators

$$H \cos(\sqrt{2\pi\eta}\Theta) \cos(\sqrt{2\pi/\eta}\Phi), \tag{34}$$

where η has been defined in Eq. (6). These operators are formally relevant and not being Lorentz scalars they belong to the class of perturbations with nonzero conformal spin. Such operators require a special treatment (see Ref. 39, Chaps. 8 and 20 and references therein). In particular, to second order, the following two spin-zero fields are generated:

$$\cos(\sqrt{8\pi\eta}\Theta), \quad \cos(\sqrt{8\pi/\eta}\Phi). \tag{35}$$

The resulting problem has been considered in detail in Chap. 20 of Ref. 39. Because we have $\eta < 1$, the renormalization-group equations flow to a sine-Gordon model in the dual field. For weak fields H, a spectral gap of order of

$$M \propto H \tag{36}$$

is generated. The gap grows with increasing magnetic field. Clearly, the growth of the gap will lead to a decrease in the transition temperature T_c—the effect observed in Cs_2CuCl_4 when the field is applied along the c direction.

There is a second way to see that application of a uniform field at an angle to the exchange anisotropy induces a spectral gap.[40] If we consider the Hamitonian

$$\mathcal{H}_{\rm ZXX,H} = J_\parallel \sum_j S_j^y S_{j+1}^y + S_j^z S_{j+1}^z + \Delta S_j^x S_{j+1}^x + H \sum_j S_j^z \tag{37}$$

and bosonize the isotropic Heisenberg chain in a field first and then take the exchange anisotropy into account as a perturbation, we obtain a sine-Gordon model for the dual field.[40,37] The cosine term in the sine-Gordon model is relevant and generates a spectral gap. The spectrum of the sine-Gordon model consists of soliton and antisoliton only and the dynamical structure factor (in the xy plane) displays an incoherent two-particle continuum. This suggests that the elementary excitations are *massive spinons*.

VI. A SINGLE SPIN-$\frac{1}{2}$ XXX CHAIN WITH DM INTERACTION

As discussed in Ref. 9, DM interactions may play a role in accounting for all the observed properties of Cs_2CuCl_4. We therefore consider now a single, isotropic spin-$\frac{1}{2}$ Heisenberg chain with a DM interaction along the z direction in spin space,

$$\mathcal{H}_{\rm DM} = J' \sum_{j=1}^{L} S_j^x S_{j+1}^x + S_j^y S_{j+1}^y + S_j^z S_{j+1}^z + D \sum_j S_j^x S_{j+1}^y - S_j^y S_{j+1}^x. \tag{38}$$

It is well known that Eq. (38) with periodic boundary conditions is equivalent to an XXZ chain with twisted boundary conditions. Indeed, a local rotation around the z axis,

$$S_j^+ = e^{-ij\theta} \tilde{S}_j^+, \quad S_j^- = e^{ij\theta} \tilde{S}_j^-, \quad S_j^z = \tilde{S}_j^z, \tag{39}$$

with $\theta = -\arctan(D/J')$ maps the Hamiltonian (38) onto

$$\mathcal{H}_{\rm DM} = J \sum_{j=1}^{L} \tilde{S}_j^x \tilde{S}_{j+1}^x + \tilde{S}_j^y \tilde{S}_{j+1}^y + \Delta \tilde{S}_j^z \tilde{S}_{j+1}^z. \tag{40}$$

Here $J = J'/\cos\theta$ and $\Delta = \cos\theta$. For a system with open boundary conditions there are no further changes. In particular, we can rest assured that bulk correlation functions in Eq. (38) can be obtained from bulk correlators in the anisotropic

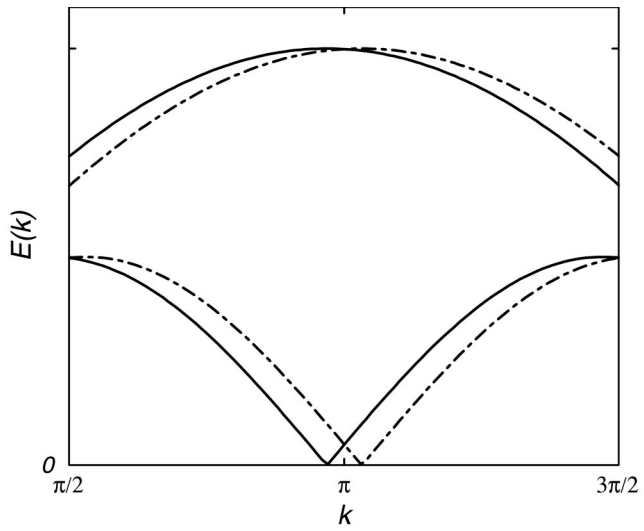

FIG. 11. Schematic two-spinon dispersion in the vicinity of $k=\pi$ in the sector $\Delta S^z=\pm 1$ for the isotropic Heisenberg chain with DM interaction.

spin-$\frac{1}{2}$ Heisenberg chain. The excitation spectrum of a spin-$\frac{1}{2}$ Heisenberg chain with DM interaction can be obtained from that of the corresponding XXZ chain by taking into account the shift in momentum induced by the mapping (39). In Fig. 11 we show the qualitative excitation spectrum with quantum numbers $\Delta S^z=\pm 1$ around momentum π. There are incommensurate soft modes at $\pi\pm\theta$. Excitations with $\Delta S^z=0$ stay commensurate, i.e., become soft at momentum π.

Using the above mapping we can now express bulk correlation functions of the spin-$\frac{1}{2}$ chain with DM interaction in terms of correlation functions of an XXZ chain with exchange $J/\cos\theta$ and anisotropy $\Delta=\cos\theta$. For example,

$$\langle S_j^+ S_{j+k}^-\rangle_{\mathrm{DM}}=e^{ik\theta}\langle \tilde{S}_j^+ \tilde{S}_{j+k}^-\rangle_{XXZ},$$
$$\langle S_j^- S_{j+k}^+\rangle_{\mathrm{DM}}=e^{-ik\theta}\langle \tilde{S}_j^- \tilde{S}_{j+k}^+\rangle_{XXZ}, \tag{41}$$

where we have used that by global spin rotational symmetry (of the bulk) around the z axis,

$$\langle \tilde{S}_j^x \tilde{S}_{j+k}^x\rangle_{XXZ}=\langle \tilde{S}_j^y \tilde{S}_{j+k}^y\rangle_{XXZ}, \quad \langle \tilde{S}_j^x \tilde{S}_{j+k}^y\rangle_{XXZ}=0. \tag{42}$$

This allows us to express the dynamical magnetic susceptibility of the model (38) in terms of the results for the Heisenberg XXZ chain,

$$\chi_{\mathrm{DM}}^{+-}(\omega,k)=\chi^{+-}(\omega,k-\theta),$$
$$\chi_{\mathrm{DM}}^{-+}(\omega,k)=\chi^{-+}(\omega,k+\theta), \tag{43}$$
$$\chi_{\mathrm{DM}}^{zz}(\omega,k)=\chi^{zz}(\omega,k).$$

In Fig. 12 we plot $-\mathrm{Im}\,\chi_{\mathrm{DM}}^{\pm\mp}(\omega,k)$ for a DM angle of $\theta=0.1$ as a function of q for four different values of $\omega/J_\parallel$ at a temperature of $k_BT/J_\parallel=0.01$. Had we plotted instead

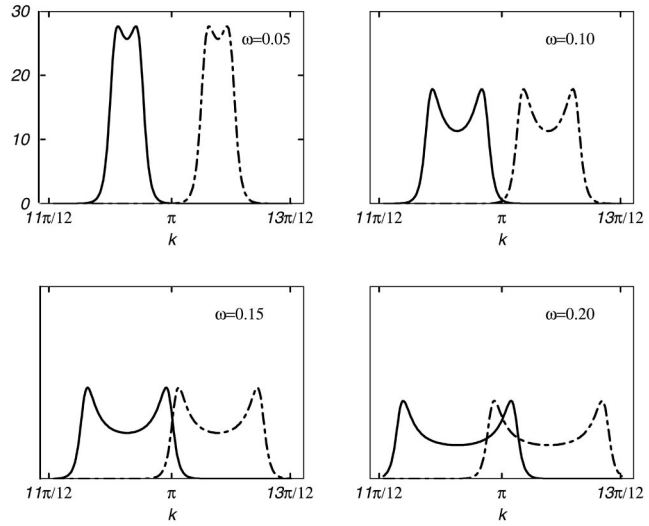

FIG. 12. Imaginary part of the dynamical susceptibility $-\mathrm{Im}\,\chi_{\mathrm{DM}}^{+-}(\omega,k)$ (full line) and $-\mathrm{Im}\,\chi_{\mathrm{DM}}^{-+}(\omega,k)$ (dashed-dotted line) as functions of q for four different values of ω/J at a temperature of $k_BT/J=0.01$. The DM angle is chosen to be $\theta=0.1$.

$$\chi^{xx}(\omega,k)=\frac{1}{4}[\chi^{+-}(\omega,k-\theta)+\chi^{-+}(\omega,k+\theta)], \tag{44}$$

we would have seen an incommensurate four-peak structure. Because of the chirality introduced by the interaction, χ_{DM}^{+-} and χ_{DM}^{-+} now differ [$\vec{u}_z\cdot\vec{S}(\vec{k})\times\vec{S}(-\vec{k})$ has a nonvanishing expectation value].

VII. DYNAMICAL SUSCEPTIBILITY FOR COUPLED HEISENBERG CHAINS WITH DM INTERACTION

In the presence of a DM interaction along the z direction in spin space, the RPA result for the dynamical susceptibility of coupled chains is given by

$$\chi_{3\mathrm{d}}^{+-}(\omega,\vec{k})=\frac{\chi^{+-}(\omega,k-\theta)}{1-J(k,k_y,k_z)\chi^{+-}(\omega,k-\theta)},$$
$$\chi_{3\mathrm{d}}^{-+}(\omega,\vec{k})=\chi_{3\mathrm{d}}^{+-}(\omega,\vec{k},\theta\to-\theta), \tag{45}$$
$$\chi_{3\mathrm{d}}^{zz}(\omega,\vec{k})=\frac{\chi^{zz}(\omega,k)}{1-2J(k,k_y,k_z)\chi^{zz}(\omega,k)},$$

where $J(k,k_y,k_z)$ is given by Eq. (17) and $\chi^{\alpha\beta}(\omega,k)$ is the dynamical susceptibility of a single Heisenberg chain. We note that the RPA expressions for $\chi_{3\mathrm{d}}^{\alpha\alpha}(\omega,\vec{k})$, $\alpha=x,y$, are not simply Eq. (16) with $\chi^{\alpha\alpha}(\omega,k)$ replaced by $\chi_{\mathrm{DM}}^{\alpha\alpha}(\omega,k)$. Instead, $\chi_{3\mathrm{d}}^{xx}=\chi_{3\mathrm{d}}^{yy}$ and $\chi_{3\mathrm{d}}^{xy}=-\chi_{3\mathrm{d}}^{yx}$ are obtained from $\chi_{3\mathrm{d}}^{+-}$ and $\chi_{3\mathrm{d}}^{-+}$ by

$$\chi_{3\mathrm{d}}^{xx}=\frac{1}{4}(\chi_{3\mathrm{d}}^{+-}+\chi_{3\mathrm{d}}^{-+}), \quad \chi_{3\mathrm{d}}^{xy}=\frac{1}{4i}(\chi_{3\mathrm{d}}^{+-}-\chi_{3\mathrm{d}}^{-+}). \tag{46}$$

In Figs. 13 and 14 we plot the imaginary parts of the dynamical susceptibilities $\chi_{3\mathrm{d}}^{+-}(\omega,k)\chi_{\mathrm{DM}}^{-+}(\omega,k)$ as functions of the

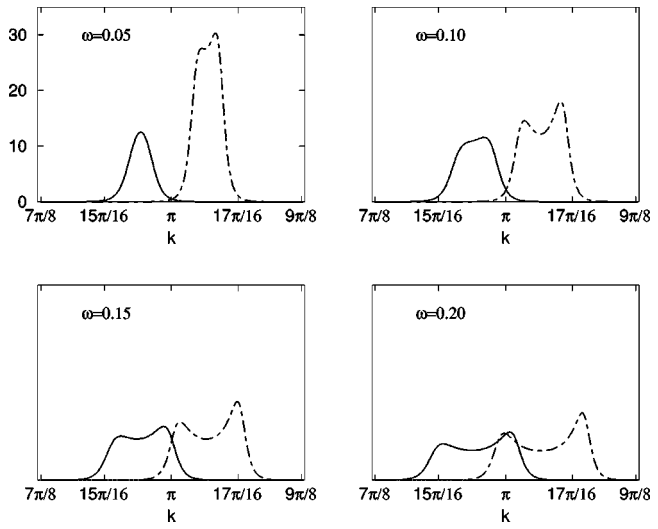

FIG. 13. $-\mathrm{Im}\,\chi^{+-}_{3d}(\omega,\vec{k})$ (solid line) and $-\mathrm{Im}\,\chi^{-+}_{3d}(\omega,\vec{k})$ (dashed-dotted line) for a DM angle $\theta=0.1$, $J_\perp/J_\parallel=0.1$, $T/J_\parallel=0.02$, and $J^z=0$. The frustrated interchain coupling breaks the symmetry around $k=\pi$.

momentum transfer along the chain direction for a DM angle of $\theta=0.1$, $J_z=0$ (the behavior for $J_z\neq 0$ is qualitatively the same) and two different values of $J_\perp$. The effect of the frustrated interchain coupling is again to remove the symmetry around $k=\pi$.

Let us now determine the transition temperature and ordering wave number in the presence of a DM interaction. We will see that the effect of the DM interaction is to significantly increase both quantities. The instability conditions read

$$J(k,k_y,k_z)\chi^{+-}(0,k-\theta)=1,$$
$$J(k,k_y,k_z)\chi^{-+}(0,k+\theta)=1, \tag{47}$$

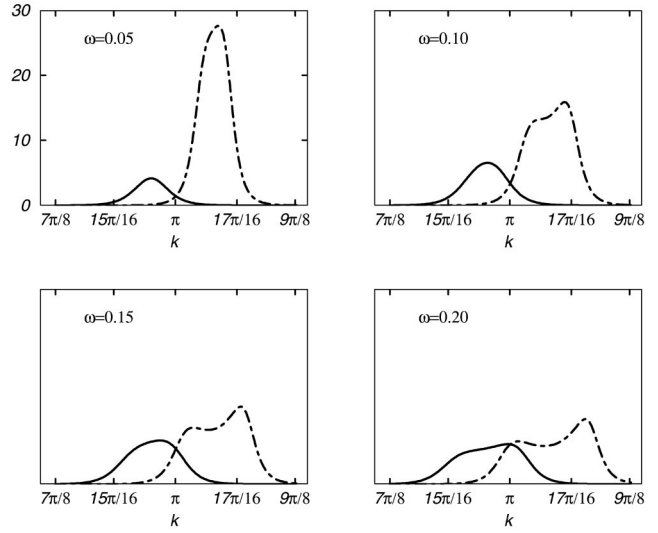

FIG. 14. $-\mathrm{Im}\,\chi^{+-}_{3d}(\omega,\vec{k})$ (solid line) and $-\mathrm{Im}\,\chi^{-+}_{3d}(\omega,\vec{k})$ (dashed-dotted line) for a DM angle of $\theta=0.1$, $J_\perp/J_\parallel=0.2$, $T/J_\parallel=0.04$, and $J^z=0$.

TABLE III. Transition temperatures $t_c=T_c/J_\parallel$ and ordering wave numbers k_0 for various values of the frustrated ($J_\perp$) interchain coupling and DM angle θ. The interplane coupling J_z is taken to be zero. The effect of a small J_z on T_c, k_0 is negligible compared to the effect of the DM interaction.

θ	$J_\perp/J_\parallel=0.1$	$J_\perp/J_\parallel=0.2$	$J_\perp/J_\parallel=0.3$
0.05	$t_c=0.008$ $k_0=0.053$	$t_c=0.017$ $k_0=0.061$	$t_c=0.028$ $k_0=0.076$
0.10	$t_c=0.016$ $k_0=0.10$	$t_c=0.032$ $k_0=0.12$	$t_c=0.051$ $k_0=0.14$
0.15	$t_c=0.023$ $k_0=0.16$	$t_c=0.046$ $k_0=0.18$	$t_c=0.073$ $k_0=0.21$
0.20	$t_c=0.031$ $k_0=0.21$	$t_c=0.060$ $k_0=0.23$	$t_c=0.095$ $k_0=0.27$

where the 1D dynamical susceptibilities fulfil $\chi^{+-}(0,k)=\chi^{-+}(0,k)$. As before the instability develops at the maximum of $J(k,k_y,k_z)\chi^{+-}(0,k\pm\theta)$. In the absence of a DM interaction ($\theta=0$) this maximum was shifted away from the maximum of the susceptibility for a single chain at $k=\pi$, because $J(k,k/2,\pi)$ vanished precisely at $k=\pi$. In the presence of a DM interaction the maxima of the single-chain susceptibility occurs at $\pi\pm\theta$ and the effect of the frustrated interchain coupling is therefore different. We find that the numerical value of k at which the instability develops is largely determined by the DM interaction and to a lesser degree by the frustration. However, the frustrated interchain coupling destroys the symmetry in momentum space around $k=\pi$ and determines whether the instability will develop in the vicinity of $\pi+\theta$ or of $\pi-\theta$. The fact that the transition temperature is increased by the DM interaction can be understood by considering the susceptibility of a single chain with DM interaction. As we have shown in Sec. VI the corresponding Hamiltonian maps onto an an anisotropic Heisenberg XXZ chain. It follows from Eq. (10) that for $\Delta<1$ the transverse susceptibility is enhanced as compared to the isotropic case $\Delta=1$, which in turn leads to a higher T_c.

Solving Eq. (47) and the equation for the maximum of $J(k,k_y,k_z)\chi^{+-}(0,k\pm\theta)$ numerically, we obtain the results for the transition temperature T_c and ordering wave number k_0 shown in Table III.

We see that a strong DM interaction leads to much larger values for T_c and k_0 than a frustrated interchain coupling alone. For the values of couplings observed in Cs_2CuCl_4 $J_\perp=0.33J$, $J_z\approx 0.05J$, $D\approx 0.05J$ we obtain $t_c=0.11$, $k_0=0.14$, which are close to the measured values. However, recent evidence suggests that the DM interaction in Cs_2CuCl_4 is not of the kind considered in this section.[19]

VIII. DM INTERACTION AND A MAGNETIC FIELD

Finally, let us investigate the case where we have both a DM interaction and a magnetic field. Now it is crucial

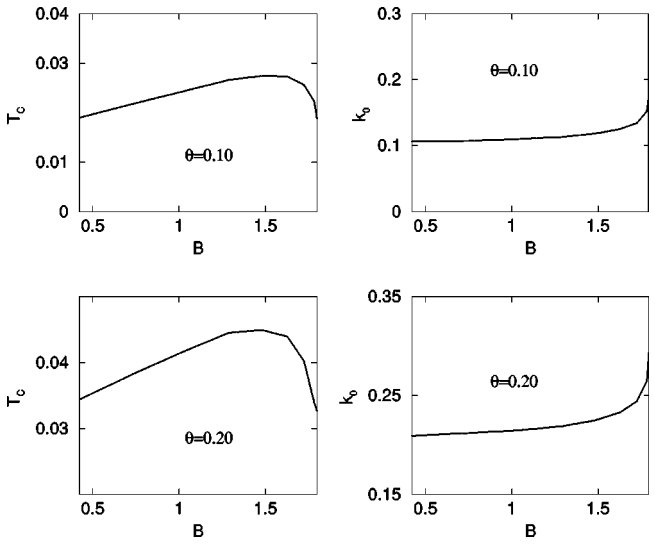

FIG. 15. Critical temperature T_c and ordering wave number k_0 as functions of the applied field $B=H/J_\parallel$ for isotropic Heisenberg chains with a DM interaction, coupled by a frustrated in-plane coupling $J_\perp=0.1J_\parallel$ and no antiferromagnetic interplane coupling $J_z=0$. The DM angle is indicated in the figures.

whether or not the field is applied along the direction singled out by the DM interaction. If it is, the system remains gapless and we can proceed along the same lines as before. If the magnetic field is applied at an angle to the DM interaction, we believe that an excitation gap is generated.[42] Let us consider the former case. The chain Hamiltonian is of the form

$$\mathcal{H}_{\mathrm{DM,H}}=J'\sum_{j=1}^{L} S_j^x S_{j+1}^x+S_j^y S_{j+1}^y+S_j^z S_{j+1}^z+D\sum_j S_j^x S_{j+1}^y - S_j^y S_{j+1}^x+H\sum_j S_j^z. \tag{48}$$

By means of the unitary transformation (39) this maps onto an anisotropic Heisenberg XXZ chain in a field

$$\mathcal{H}_{\mathrm{DM,H}}=J\sum_{j=1}^{L} \tilde{S}_j^x\tilde{S}_{j+1}^x+\tilde{S}_j^y\tilde{S}_{j+1}^y+\Delta\tilde{S}_j^z\tilde{S}_{j+1}^z+H\sum_j \tilde{S}_j^z, \tag{49}$$

where $J=J'/\cos\theta$ and $\Delta=\cos\theta$ [$\theta=-\arctan(D/J')$ as before]. The model (49) remains gapless and we can determine the finite temperature dynamical susceptibility by the same methods we used in the absence of a DM interaction in Sec. V above. The result for the transverse susceptibility is of the form (27), where the exponent $\eta(H,D)$ and velocity $u(H,D)$ can again be determined from the Bethe Ansatz, whereas the amplitude $A_x(H)$ is known numerically.[38] Taking the interchain couplings into account in RPA and then looking for instabilities as before, we obtain the results shown in Fig. 15.

The behavior of $T_c(H)$ and $k_0(H)$ as functions of the applied field is similar to what we found in the absence of a DM interaction. However, like for the zero-field case a strong DM interaction leads to a significant increase in the absolute values of T_c and k_0.

IX. GENERAL DZYALOSHINSKII-MORIYA INTERACTION

In this section we discuss how to treat more general types of DM interactions within the framework of our coupled chain approach.

A. Dzyaloshinskii-Morya interaction along the chains

In a compound such as Cs_2CuCl_4, the three-dimensional elementary cell contains four Cu^{2+} ions.[41] Two of them, say (1) and (2), lie within a planar layer and are coupled by a relatively strong, frustrated exchange interaction. The other two, say (3) and (4), lie in the layer above and are coupled weakly to (1) and (2).[9]

In the case where it involves spins along the chain direction, the most general form of the DM interaction which is allowed by symmetries[9] is

$$\mathcal{I}_{\mathrm{DM}}=\sum_{n,m}\vec{D}_1\cdot[\vec{S}^{(1)}_{n,m}\times\vec{S}^{(1)}_{n+1,m}]+\vec{D}_2\cdot\left[\vec{S}^{(2)}_{n,m+\frac{1}{2}}\times\vec{S}^{(2)}_{n+1,m+\frac{1}{2}}\right]. \tag{50}$$

Generically, this interaction requires the distinction between the sets (1) and (2). (Up to now, we had only considered the case $\vec{D}_1=\vec{D}_2$.)

As a consequence, and from now on, the Heisenberg chains forming up the triangular planar lattice will not necessarily be considered all equivalent, but belonging alternatively to sets (1) or (2). This doubles the primitive cell chosen in Fig. 5 in the y direction. The magnetic Hamiltonian that takes the difference between the two types of spins into account is

$$\mathcal{H}_{\mathrm{DM}}=J_\parallel\sum_{m,n}\vec{S}^{(1)}_{n,m}\cdot\vec{S}^{(1)}_{n+1,m}+\vec{S}^{(2)}_{n,m+1/2}\cdot\vec{S}^{(2)}_{n+1,m+1/2} +J_\perp\sum_{m,n}\vec{S}^{(1)}_{n,m}\cdot(\vec{S}^{(2)}_{n,m+1/2}+\vec{S}^{(2)}_{n,m-1/2}) +J_\perp\sum_{m,n}\vec{S}^{(2)}_{n,m+1/2}\cdot(\vec{S}^{(1)}_{n+1,m}+\vec{S}^{(1)}_{n-1,m+1})+\mathcal{I}_{\mathrm{DM}}. \tag{51}$$

Due to the doubling in the y direction, the Fourier transform of the interchain spin-spin couplings is now

$$J(\vec{k})=2J_\perp[\cos(k_y/2)+\cos(k_x-k_y/2)]. \tag{52}$$

In order to choose the quantization axes for sets (1) and (2) we introduce the unit vectors

$$\vec{u}_1=\vec{D}_1/|\vec{D}_1|,\quad \vec{u}_2=\vec{D}_2/|\vec{D}_2|, \tag{53}$$

$$\vec{v}=\vec{u}_1\times\vec{u}_2/|\vec{u}_1\times\vec{u}_2|. \tag{54}$$

The spins along the chains of type (1) and (2) will be quantized in local coordinate systems with axes $(\vec{v},\vec{u}_1\times\vec{v},\vec{u}_1)$ and $(\vec{v},\vec{u}_2\times\vec{v},\vec{u}_2)$, respectively. We denote the angle between $\vec{u}_1$ and $\vec{u}_2$ by ζ and define two DM angles by $\theta_1 = -\arctan(|\vec{D}_1|/J_\parallel)$, $\theta_2 = -\arctan(|\vec{D}_2|/J_\parallel)$.

Specializing to Cs_2CuCl_4, we note that the space symmetry group for this material is $Pnma$. This group contains symmetry elements which map the spin chains of different types onto each other, which leads to the following restrictions of the DM vectors $\vec{D}_1$ and $\vec{D}_2$. They are perpendicular to the chain direction, perpendicular to each other and of equal length. This yields that $\theta_1=\theta_2$ in this case; see Ref. 9 for a detailed symmetry analysis.

Next we define the usual step operators for $j=1,2$:

$$S^{\pm}_{(j)} = S^x_{(j)} \pm i S^y_{(j)}. \tag{55}$$

Notice that because of our choice of the quantization axis, the letters x,y,z refer to different directions for $j=1$ and $j=2$. In Fourier space, the total Hamiltonian is

$$\begin{aligned}\mathcal{H}_{\rm DM} &= J_\parallel \sum_{\vec{k};j=1,2} \frac{\cos(k_x-\theta_j)}{\cos\theta_j} S^+_{(j)}(\vec{k}) S^-_{(j)}(-\vec{k}) \\ &+ J_\parallel \sum_{\vec{k};j=1,2} \cos k_x S^z_{(j)}(\vec{k}) S^z_{(j)}(-\vec{k}) + \cos\zeta \sum_{\vec{k}} J(\vec{k}) \\ &\times [S^y_{(1)}(\vec{k}) S^y_{(2)}(-\vec{k}) + S^z_{(1)}(\vec{k}) S^z_{(2)}(-\vec{k})] \\ &+ \sin\zeta \sum_{\vec{k}} J(\vec{k}) [S^z_{(1)}(\vec{k}) S^y_{(2)}(-\vec{k}) - S^y_{(1)}(\vec{k}) S^z_{(2)}(-\vec{k})] \\ &+ \sum_{\vec{k}} J(\vec{k}) S^x_{(1)}(\vec{k}) S^x_{(2)}(-\vec{k}).\end{aligned} \tag{56}$$

Next we will write the ''effective'' quadratic spin Hamiltonian corresponding to the random-phase approximation. In order to do so, we define

$$\begin{aligned}\Sigma_j &= \frac{1}{2}\{[\chi^{xx}_j(k_x+\theta_j)]^{-1} + [\chi^{xx}_j(k_x-\theta_j)]^{-1}\}, \\ \Delta_j &= \frac{1}{2i}\{[\chi^{xx}_j(k_x+\theta_j)]^{-1} - [\chi^{xx}_j(k_x-\theta_j)]^{-1}\}, \\ \Omega_j &= [\chi^{zz}_j(k_x)]^{-1}.\end{aligned} \tag{57}$$

Here χ^{xx}_j and χ^{zz}_j denote the time-ordered imaginary-time correlation functions for chain (j) in the presence of the DM interaction with coupling $\vec{D}_j$. They are related to the transverse and longitudinal dynamical susceptibilities for chain (j) by a Wick rotation and a global minus sign.

The effective RPA correlation functions between spin operators $(S^x_1,S^y_1,S^z_1,S^x_2,S^y_2,S^z_2)(\vec{k})$ and spin operators $(S^x_1,S^y_1,S^z_1,S^x_2,S^y_2,S^z_2)^t(-\vec{k})$ are then given by the inverse of the bilinear form

$$\begin{bmatrix} \Sigma_1 & \Delta_1 & 0 & J & 0 & 0 \\ -\Delta_1 & \Sigma_1 & 0 & 0 & J\cos\zeta & J\sin\zeta \\ 0 & 0 & \Omega_1 & 0 & -J\sin\zeta & J\cos\zeta \\ J & 0 & 0 & \Sigma_2 & \Delta_2 & 0 \\ 0 & J\cos\zeta & -J\sin\zeta & -\Delta_2 & \Sigma_2 & 0 \\ 0 & J\sin\zeta & J\cos\zeta & 0 & 0 & \Omega_2 \end{bmatrix}. \tag{58}$$

The emergence of a pole in the dynamical susceptibility corresponds to the vanishing of the determinant of this matrix. This leads to the following necessary condition:

$$\begin{aligned}0 &= J^6 - [(1+\cos^2\zeta)\Sigma_1\Sigma_2 + \sin^2\zeta(\Sigma_1\Omega_2+\Sigma_2\Omega_1) \\ &+ \Omega_1\Omega_2\cos^2\zeta - 2\Delta_1\Delta_2\cos\zeta]J^4 + \{(1+\cos^2\zeta) \\ &\times \Omega_1\Omega_2\Sigma_1\Sigma_2 + \sin^2\zeta[\Omega_1\Sigma_1(\Sigma_2^2+\Delta_2^2) \\ &+ \Omega_2\Sigma_2(\Sigma_1^2+\Delta_1^2)] + \cos^2\zeta(\Sigma_1^2+\Delta_1^2)(\Sigma_2^2+\Delta_2^2) \\ &- 2\Omega_1\Omega_2\Delta_1\Delta_2\cos\zeta\}J^2 - \Omega_1\Omega_2(\Sigma_1^2+\Delta_1^2)(\Sigma_2^2+\Delta_2^2).\end{aligned} \tag{59}$$

In the particular case when $\vec{u}_1=\vec{u}_2$, but θ_1 is not necessarily equal to θ_2, the condition simplifies to

$$\begin{aligned}0 &= [1-J^2\chi^{zz}_1(k)\chi^{zz}_2(k)][1-J^2\chi^{xx}_1(k+\theta_1)\chi^{xx}_2(k+\theta_2)] \\ &\times [1-J^2\chi^{xx}_1(k-\theta_1)\chi^{xx}_2(k-\theta_2)],\end{aligned} \tag{60}$$

where k stands for k_x. If in addition to $\vec{u}_1=\vec{u}_2$ we also have $\theta_1=\theta_2$ then we recover, as we must, the instability conditions discussed before. The dynamical susceptibilities can be calculated, by inverting Eq. (58), then continuing analytically on the frequencies.

B. Dzyaloshinskii-Moriya interaction along the interchain bonds

Up to this point we have only considered the case when the DM interaction involves spin along the chains. It was recently suggested to us by R. Coldea and A. Tennant[19] that the DM interaction in Cs_2CuCl_4 may also involve pairs of spin along the interchain couplings.

The direction of the DM vector in this case is again constrained by crystal symmetries.[19] The DM vector is perpendicular to the triangular planes and is staggered along the chain direction as shown in Fig. 16.

For Cs_2CuCl_4 the DM vector appears to be staggered between triangular layers as well.[19] In what follows we will first consider the simpler case in which there is no staggering between layers in order to keep our formulas simple.

We again need to distinguish between spin chains of type (1) and (2). The calculations are similar to the ones of Sec. IX A. Since the longitudinal spin operators $S^z_{(j)}$ do not couple to the transverse ones, the transverse and longitudinal susceptibilities can be calculated separately. In Fourier space, the Hamiltonian takes the form

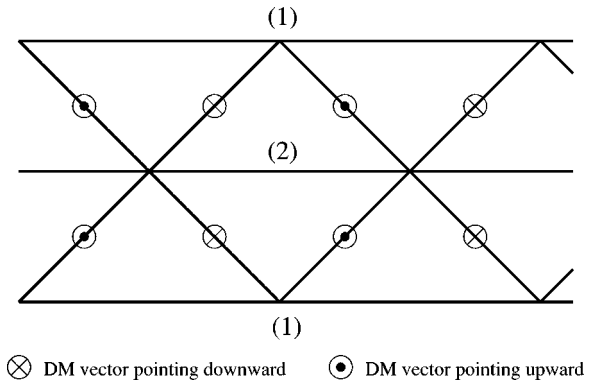

FIG. 16. Schematic representation of the orientation of the allowed directions of the DM vector within one layer for the case where the interaction involves spins along the interchain bonds.

$$\mathcal{H}_{\mathrm{DM}}=\mathcal{H}_0+\mathcal{H}_{\mathrm{int}},$$

$$\mathcal{H}_0=J_{\parallel}\sum_{\vec{k};j=1,2}\sum_{\alpha}\cos k_x S^{\alpha}_{(j)}(\vec{k})S^{\alpha}_{(j)}(-\vec{k}),$$

$$\mathcal{H}_{\mathrm{int}}=\sum_{\vec{k}}\vec{\mathcal{S}}(\vec{k})^T A(\vec{k})\vec{\mathcal{S}}^{\dagger}(-\vec{k})+\sum_{\vec{k}}2\tilde{J}(\vec{k})S^z_{(1)}(\vec{k})S^z_{(2)}(-\vec{k})$$

$$+\sum_{\vec{k}}\sum_{j=1,2}J_z\cos k_z S^z_{(j)}(\vec{k})S^z_{(j)}(-\vec{k}), \tag{61}$$

where D denotes the DM coupling,

$$\vec{\mathcal{S}}(\vec{k})^T=[S^+_{(1)}(\vec{k}),S^+_{(2)}(\vec{k})],$$

$$\tilde{J}(\vec{k})=J_{\perp}[\cos(k_y/2)+\cos(k_x-k_y/2)], \tag{62}$$

$$K(\vec{k})=D[\sin(k_y/2)+\sin(k_x-k_y/2)],$$

and $A(\vec{k})$ is the 2×2 matrix

$$\begin{bmatrix} J_z\cos k_z & \tilde{J}+K \\ \tilde{J}+K & J_z\cos k_z \end{bmatrix}. \tag{63}$$

It will be convenient to define

$$L_{\theta}(\vec{k})=\tilde{J}(\vec{k})+K(\vec{k})$$

$$=\frac{J_{\perp}}{\cos\theta}\left[\cos\left(\frac{k_y}{2}+\theta\right)+\cos\left(k_x-\frac{k_y}{2}+\theta\right)\right], \tag{64}$$

where $\theta=-\arctan(D/J_{\perp})$.

We denote by $\chi^{+-}(\vec{k})\equiv\chi^{-+}(\vec{k})$ the time-ordered imaginary-time transverse correlation function between spins $S^+_{(j)}(\vec{k})$ and spin $S^-_{(j)}(-\vec{k})$ in the absence of the interchain coupling and DM interaction. This is of course simply the correlation function of a single one-dimensional chain.

The RPA expressions for the transverse correlation functions between spin operators $\mathcal{S}_{\alpha}(\vec{k})$ and $\mathcal{S}^{\dagger}_{\beta}(-\vec{k})$ $(\alpha,\beta=1,2)$ are given by the matrix elements of the inverse of the following 2×2 matrix:

$$\begin{bmatrix} [\chi^{+-}]^{-1}+J_z\cos k_z & L_{\theta} \\ L_{\theta} & [\chi^{+-}]^{-1}+J_z\cos k_z \end{bmatrix}. \tag{65}$$

The time-ordered imaginary-time two point correlation function of spins is obtained by adding the contributions from the various sublattice correlators, i.e., by taking, e.g.,

$$\frac{1}{2}\sum_{j,l}\langle S^+_{(j)}(\vec{k})S^-_{(l)}(-\vec{k})\rangle. \tag{66}$$

After analytic continuation we obtain the following RPA formula for the transverse dynamical susceptibilities:

$$\chi^{+-}_{3d}(\omega,\vec{k})=\frac{\chi^{+-}(\omega,k_x)}{1-[L_{\theta}(\vec{k})+J_z\cos k_z]\chi^{+-}(\omega,k_x)},$$

$$\chi^{-+}_{3d}(\omega,\vec{k})=\chi^{+-}_{3d}(\omega,-\vec{k}). \tag{67}$$

Here $\chi^{+-}(\omega,k_x)$ is the dynamical susceptibility of a single one-dimensional chain. We note that we could have arrived at this result by first removing the DM interaction along the interchain bonds by means of a unitary transformation in a way analogous to Eq. (39). This induces an effective DM interaction along the chains and the resulting Hamiltonian can again be analyzed within RPA. After undoing the unitary transformation one recovers Eq. (67).

The structure of the dynamical susceptibilities (67) is quite similar to the one we obtained in the case where the DM interaction is along the chain direction (45). There again is an effective global shift of the momentum by a ''DM angle'' θ. However, now the angle depends on the ratio of the DM coupling D to the interchain coupling $J_{\perp}$ rather than the strong exchange $J_{\parallel}$, which makes it much larger. This leads to an enhancement of the effect of the DM interaction.

The condition for the emergence of a transverse instability towards the formation of a coherent mode reads

$$1=\max_{\vec{k}}\{[L_{\theta}(\vec{k})+J_z\cos k_z]\chi^{+-}(\omega,k_x)\}. \tag{68}$$

One finds that the instability again occurs along the chain direction, i.e., $k_y=k_x$.

C. Taking into account the staggered layers

It was suggested in Ref. 19 that in Cs_2CuCl_4 the direction of the DM vector alternates between neighboring layers. This feature can be accomodated within our calculation as follows.

Let us first suppose that the interlayer coupling constant J^z is negligible. Then the global transverse dynamical susceptibilities are given by the sums over the contributions from the two types of layers. In this case the transverse susceptibility reads

$$\chi_{3d}^{+-}(\omega,\vec{k}) = \frac{\chi^{+-}(\omega,k_x)[1-J(\vec{k})\chi^{+-}(\omega,k_x)]}{[(1-L_\theta(\vec{k})\chi^{+-}(\omega,k_x)][1-L_{-\theta}(\vec{k})\chi^{+-}(\omega,k_x)]}, \quad \chi_{3d}^{-+}(\omega,\vec{k}) = \chi_{3d}^{+-}(\omega,\vec{k}). \tag{69}$$

As expected the transverse dynamical susceptibility has lost its chiral nature, i.e., we now have $\chi_{3d}^{-+}=\chi_{3d}^{+-}$. This is in marked contrast to the case where the DM interaction involves spins along the chains, for which we always had $\chi_{3d}^{-+}\neq\chi_{3d}^{+-}$.

If J_z is not zero the calculations are slightly more complicated. One has now to distinguish spins in neighboring layers and the elementary cell is doubled in the z direction. We will denote the spin operators corresponding to the four sites per unit cell by $S_{(j,k)}^{\alpha}$ $(j,k=1,2)$. Let us also introduce the function $I(\vec{k})=J^z\cos(k_z/2)$. Then the effective RPA transverse correlation functions between spin operators $(S_{(1,1)}^{+},S_{(2,1)}^{+},S_{(1,2)}^{+},S_{(2,2)}^{+})(\vec{k})$ and $(S_{(1,1)}^{-},S_{(2,1)}^{-},S_{(1,2)}^{-},S_{(2,2)}^{-})^T(-\vec{k})$ are given by the inverse of the following bilinear form:

$$\begin{bmatrix} [\chi^{+-}]^{-1} & L_\theta & I & 0 \\ L_\theta & [\chi^{+-}]^{-1} & 0 & I \\ I & 0 & [\chi^{+-}]^{-1} & L_{-\theta} \\ 0 & I & L_{-\theta} & [\chi^{+-}]^{-1} \end{bmatrix}. \tag{70}$$

The time-ordered imaginary-time two point function of spin operators is again obtained by summing over the sublattice contributions. After analytic continuation, we obtain the following RPA expression for the transverse dynamical susceptibility:

$$\chi_{3d}^{+-}(\omega,\vec{k}) = \frac{\chi^{+-}(\omega,k_x)[1+N_1(\vec{k})\chi^{+-}(\omega,k_x)]}{\{1-2\tilde{J}(\vec{k})\chi^{+-}(\omega,k_x)+N_2(\vec{k})[\chi^{+-}(\omega,k_x)]^2\}}, \tag{71}$$

where

$$N_1(\vec{k}) = I(\vec{k}) - \tilde{J}(\vec{k}), \quad N_2(\vec{k}) = \tilde{J}^2(\vec{k}) - K^2(\vec{k}) - I^2(\vec{k}). \tag{72}$$

We again have that

$$\chi_{3d}^{-+}(\omega,\vec{k}) = \chi_{3d}^{+-}(\omega,\vec{k}). \tag{73}$$

From Eq. (71) we obtain a modified set of instability conditions

$$(J(\vec{k}) \pm \sqrt{K^2(\vec{k})+I^2(\vec{k})})\chi^{+-}(0,k_x)=1. \tag{74}$$

Extremizing with respect to k_z and k_y yields the conditions $k_y=k_x$ and $k_z=0$.

If we specify the exchange couplings according to the values suggested for Cs_2CuCl_4 ($J_z\simeq 0.05J_\parallel$, $J_\perp \simeq 0.33J_\parallel$, $D\simeq 0.05J_\parallel$) we obtain a critical temperature of $T_c=0.727$ K and an ordering wave number of $k_0=0.154$. These are close to the experimental values $T_c=0.62$ K and $k_0=0.186$ (see Table IV).

TABLE IV. Transition temperatures $t_c=T_c/J_\parallel$ and ordering wave numbers k_0 for various values of the frustrated ($J_\perp$) interchain coupling and interchain DM angle $\theta=\arctan(D/J_\perp)$. The interplane coupling J_z is taken to be $0.05J_\parallel$.

θ	$J_\perp/J_\parallel=0.1$	$J_\perp/J_\parallel=0.2$	$J_\perp/J_\parallel=0.3$
0.05	$t_c=0.070$ $k_0=0.021$	$t_c=0.078$ $k_0=0.046$	$t_c=0.092$ $k_0=0.082$
0.10	$t_c=0.074$ $k_0=0.022$	$t_c=0.091$ $k_0=0.053$	$t_c=0.120$ $k_0=0.103$
0.15	$t_c=0.079$ $k_0=0.023$	$t_c=0.109$ $k_0=0.062$	$t_c=0.153$ $k_0=0.128$
0.20	$t_c=0.087$ $k_0=0.025$	$t_c=0.130$ $k_0=0.073$	$t_c=0.189$ $k_0=0.153$

X. SUMMARY AND CONCLUSIONS

In this work we have studied the dynamical response of frustrated quasi-1D spin-$\frac{1}{2}$ Heisenberg magnets in the disordered phase. The starting point of our approach are exact results for the finite-temperature dynamical susceptibility of an ensemble of uncoupled chains. Taking the couplings between chains into account within the framework of a random-phase approximation, we obtained an analytic expression for the dynamical structure factor of the quasi-1D system we are interested in. In the disordered phase the main effects of the frustration are to generate an *asymmetry* of the line shape and a shift of the apparent dispersion to an incommensurate wave vector.

By analyzing the instability of the disordered phase with respect to the formation of collective modes we studied the transition to the low-temperature ordered phase. In particular we determined the ordering temperature and ordering wave vector within the framework of our approach. We found that there is a very weak instability towards an incommensurately ordered state.

We then considered the effects of an applied magnetic field. We found that for isotropic Heisenberg magnets application of a magnetic field leads first to an increase in the transition temperature $T_c(H)$ and for very large field to an eventual decrease. In the presence of an exchange anisotropy we found two distinct behaviors: if the field is applied along the direction of the anisotropy the situation is very similar to the isotropic case. Applying the field at an angle to the anisotropy generates a gap in the individual chains, which leads to a decrease of $T_c(H)$ with H in the quasi-1D system. This type of magnetic phase diagram is qualitatively similar to what has been observed in Cs_2CuCl_4.

In the second part of this work we took into account the effects of various types of Dzyaloshinskii-Moriya interac-

tions, which break spin rotational invariance. We first considered DM interactions involving spins along the chain directions and then DM interactions involving spins along interchain bonds. In the disordered phase the main effect of DM interactions is to generate stronger incommensurations. DM interactions also leads to a significant enhancement in the transition temperature and ordering wave number.

In general our results are qualitatively similar to what is observed experimentally in Cs_2CuCl_4. In presence of a DM interaction of the kind proposed in Ref. 19 for Cs_2CuCl_4 we obtain a transition temperature and ordering wave number, which are close to the experimental values. However, given that the interchain coupling is not small it is unclear how reliable the RPA approach is. In light of this fact it would be very interesting to determine the leading corrections to RPA, which can be done for example along the lines of Ref. 36. It also would be interesting to extend the coupled chains approach to the ordered phase. This is not straightforward due to the presence of ''twist'' operators.[17]

ACKNOWLEDGMENTS

We thank Radu Coldea and Alan Tennant for many stimulating discussions and explaining their experimental results to us. This work was supported by the EPSRC under grants AF/100201 (F.H.L.E.) and GR/N19359 (M.B. and F.H.L.E.).

[1] D. A. Tennant, R. A. Cowley, S. E. Nagler, and A. M. Tsvelik, Phys. Rev. B **52**, 13 368 (1995); D. C. Dender, P. R. Hammar, D. H. Reich, C. Broholm, and G. Aeppli, Phys. Rev. Lett. **79**, 1750 (1997).

[2] D. A. Tennant, S. E. Nagler, D. Welz, G. Shirane, and K. Yamada, Phys. Rev. B **52**, 13 381 (1995).

[3] B. Lake, D. A. Tennant, and S. E. Nagler, Phys. Rev. Lett. **85**, 832 (2000).

[4] R. Coldea, D. A. Tennant, A. M. Tsvelik, and Z. Tylczynski, Phys. Rev. Lett. **86**, 1335 (2001).

[5] S. A. Brazovskii and V. M. Yakovenko, Zh. Éksp. Teor. Fiz. **89**, 2318 (1985) [Sov. Phys. JETP **62**, 1340 (1985)].

[6] F. H. L. Essler, A. M. Tsvelik, and G. Delfino, Phys. Rev. **56**, 11 001 (1997).

[7] R. Coldea, D. A. Tennant, R. A. Cowley, D. F. McMorrow, B. Dorner, and Z. Tylczynski, J. Phys.: Condens. Matter **8**, 7473 (1996); R. Coldea, D. A. Tennant, R. A. Cowley, D. F. McMorrow, B. Dorner, and Z. Tylczynski, J. Magn. Magn. Mater. **177**, 659 (1998).

[8] R. Coldea, D. A. Tennant, R. A. Cowley, D. F. McMorrow, B. Dorner, and Z. Tylczynski, Phys. Rev. Lett. **79**, 151 (1997).

[9] R. Coldea, Ph.D. thesis, Oxford University, 1997.

[10] M. F. Collins and O. A. Petrenko, Can. J. Phys. **75**, 605 (1997).

[11] I. A. Zaliznyak, C. Broholm, M. Kibune, M. Nohara, H. Takagi, Phys. Rev. Lett. **83**, 5370 (1999); M. Matsuda and K. Katsumata, J. Magn. Magn. Mater. **140**, 1617 (1995); Z. Hiroi, M. Azuma, M. Takano, and Y. Bando, J. Solid State Chem. **95**, 230 (1991); N. Motoyama, H. Eisaki, and S. Uchida, Phys. Rev. Lett. **76**, 3212 (1996).

[12] A. V. Chubukov, S. Sachdev, and T. Senthil, Nucl. Phys. B **426**, 601 (1994); P. Azaria, P. Lecheminant, and D. Mouhanna, *ibid.* **455**, 648 (1995).

[13] R. R. P. Singh, O. A. Starykh, and P. J. Freitas, J. Appl. Phys. **83**, 7387 (1998).

[14] Z. Weihong, R. H. McKenzie, and R. R. P. Singh, Phys. Rev. B **59**, 14 367 (1999).

[15] C. H. Chung, J. B. Marston, and R. H. McKenzie, J. Phys.: Condens. Matter **13**, 5159 (2001).

[16] R. Moessner, Conference on Highly Frustrated Magnetism (HFM-2000), Waterloo, 2000 (unpublished), and references therein.

[17] A. A. Nersesyan, A. O. Gogolin, and F. H. L. Essler, Phys. Rev. Lett. **81**, 910 (1998).

[18] S. R. White and I. Affleck, Phys. Rev. B **54**, 9862 (1996); D. Allen and D. Sénéchal, *ibid.* **55**, 299 (1997); A. A. Zvyagin, *ibid.* **57**, 1035 (1998); Z. Weihong, V. Kotov, and J. Oitmaa, *ibid.* **57**, 11 439 (1998); P. Azaria, P. Lecheminant, and A. A. Nersesyan, *ibid.* **58**, R8881 (1998); A. K. Kolezhuk and H.-J. Mikeska, Int. J. Mod. Phys. B **5**, 2325 (1998); D. Allen, F. H. L. Essler, and A. A. Nersesyan, Phys. Rev. B **61**, 8871 (2000); D. C. Johnston *et al.*, *ibid.* **61**, 9558 (2000); D. Cabra, A. Honecker, and P. Pujol, Eur. Phys. J. B **13**, 55 (2000); A. A. Aligia, C. D. Batista, and F. H. L. Essler, Phys. Rev. B **62**, 3259 (2000); A. K. Kolezhuk, *ibid.* **62**, R6057 (2000); Y. Nishiyama, Eur. Phys. J. B **17**, 295 (2000); P. Azaria and P. Lecheminant, Nucl. Phys. B **575**, 439 (2000); A. A. Zvyagin, Low Temp. Phys. **26**, 134 (2000); M. E. Zhitomirsky, A. Honecker, and O. A. Petrenko, Phys. Rev. Lett. **85**, 3269 (2000); R. Chitra and R. Citro, Phys. Rev. B **63**, 054 441 (2001); D. C. Cabra, A. Dobry, and G. L. Rossini, Phys. Rev. B **63**, 144408 (2001).

[19] R. Coldea and D. A. Tennant (private communication).

[20] L. D. Faddeev and L. Takhtajan, J. Sov. Math. **24**, 241 (1984).

[21] H. Bethe, Z. Phys. **71**, 205 (1931); C. N. Yang and C. P. Yang, Phys. Rev. **150**, 321 (1966).

[22] V. E. Korepin, A. G. Izergin, and N. M. Bogoliubov, *Quantum Inverse Scattering Method, Correlation Functions and Algebraic Bethe Ansatz* (Cambridge University Press, Cambridge, England, 1993).

[23] A. Luther and I. Peschel, Phys. Rev. B **9**, 2911 (1974); **12**, 3908 (1975).

[24] H. J. Schulz and C. Bourbonnais, Phys. Rev. B **27**, 5856 (1983); H. J. Schulz, *ibid.* **34**, 6372 (1986).

[25] S. Lukyanov, Nucl. Phys. B **522**, 533 (1998).

[26] I. Affleck, J. Phys. A **31**, 4573 (1998).

[27] V. Barzykin, J. Phys.: Condens. Matter **12**, 2053 (2000).

[28] S. Lukyanov and A. B. Zamolodchikov, Nucl. Phys. B **493**, 571 (1997).

[29] V. Barzykin, Phys. Rev. B **63**, 140412(R) (2001).

[30] A. W. Sandvik, Phys. Rev. Lett. **83**, 3069 (1999).

[31] H. J. Schulz, G. Cuniberti, and P. Pieri, in *Field Theories for Low-Dimensional Matter Systems*, Lecture Notes of the Chia Laguna Summer School, Italy, 1997, edited by G. Morandi *et al.* (Springer, Berlin, 2000).

[32] A. M. Tsvelik, *Quantum Field Theory for Condensed Matter Physics* (Cambridge University Press, Cambridge, England, 1995).
[33] S. Lukyanov, Phys. Rev. B **59**, 11 163 (1999).
[34] D. J. Scalapino, Y. Imry, and P. Pincus, Phys. Rev. B **11**, 2042 (1975).
[35] H. J. Schulz, Phys. Rev. Lett. **77**, 2790 (1996).
[36] V. Y. Irkhin and A. A. Katanin, Phys. Rev. B **61**, 6757 (2000).
[37] F. H. L. Essler, Phys. Rev. B **59**, 14 376 (1999).
[38] T. Hikihara and A. Furusaki, Phys. Rev. B **63**, 134438 (2001).
[39] A. O. Gogolin, A. A. Nersesyan, and A. M. Tsvelik, *Bosonization and Strongly Correlated Systems* (Cambridge University Press, Cambridge, England, 1998).
[40] A. A. Nersesyan (private communication).
[41] S. Bailleul, D. Svornos, P. Porcher, and A. Tomas, C. R. Acad. Sci., Ser. II: Mec., Phys., Chim., Sci. Terre Univers. **313**, 1149 (1991).
[42] M. Bocquet and F. H. L. Essler (unpublished).